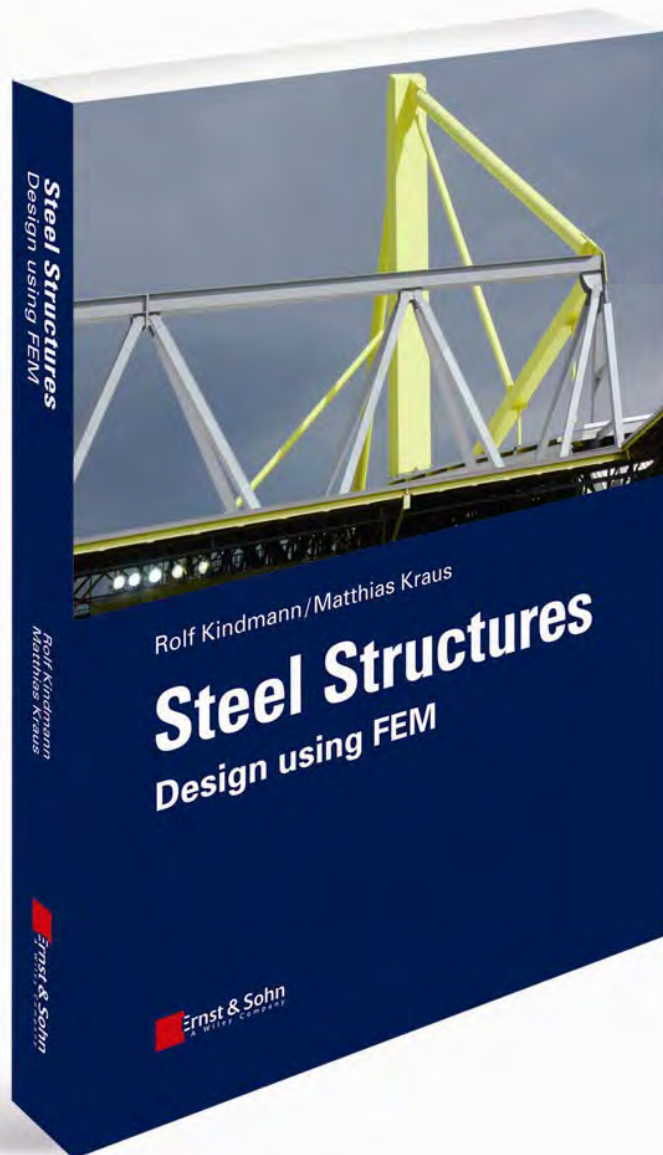# Sample Chapter

Steel Structures – Design using FEM
Rolf Kindmann, Matthias Kraus
Copyright © 2011 Ernst & Sohn, Berlin
ISBN: 978-3-433-02978-7

10 FEM for Plane Load-Bearing Structures

10.1 Plates with Lateral and In-Plane Loading

Plane load bearing structures are structural members with a proportionately small thickness compared to the length and width. Due to their thinness, it is sufficient to consider their midplane. This is comparable with the reduction of a beam member to its member axis. As shown in Figure 10.1, regarding plane load-bearing structures, plates with different loadings are distinguished: Plates with **loads acting in-plane** and **loads acting laterally to the plane**. Typical examples for plates loaded in-plane are walls and for plates laterally loaded slabs, however, usually walls and slabs are massive structural members and not steel constructions. Plates made of steel are dealt with in detail in Chapter 10.6.
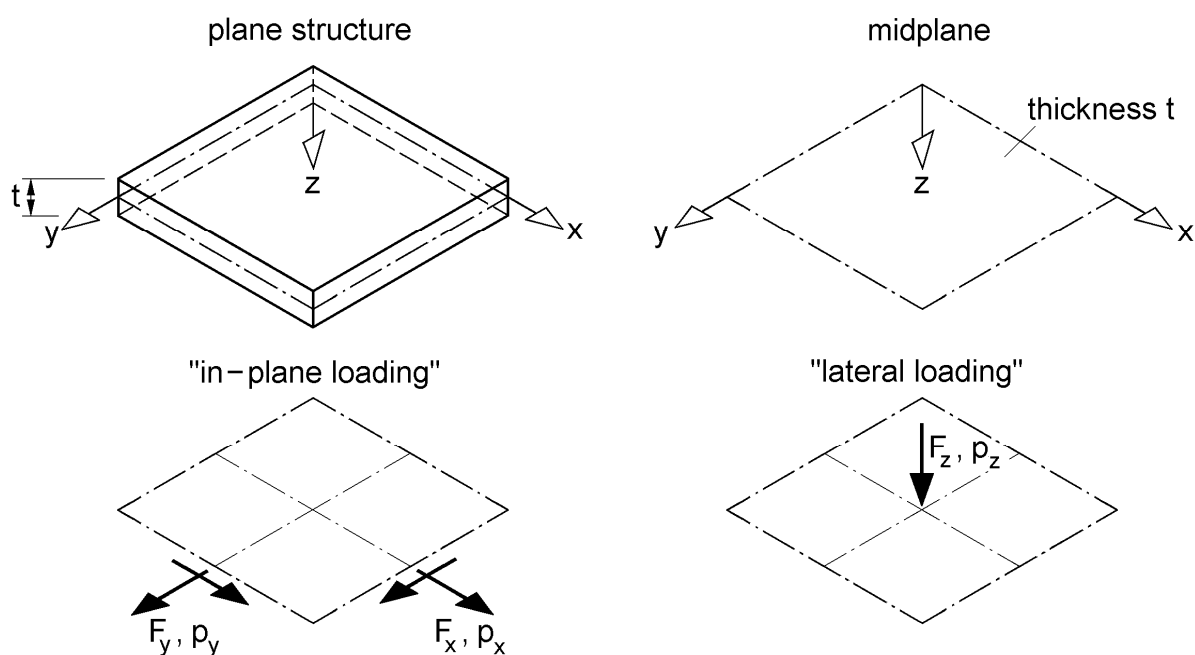

Figure 10.1   Plane structures as plates with in-plane and lateral loading

10.2 Stresses and Internal Forces

Figure 10.2 contains the definition of the stresses for plane structures. For reasons of clarity, only the stresses at the positive intersection x = const. and y = const. are depicted. The figure shows merely the directions and designations without regarding the equilibrium of the element.
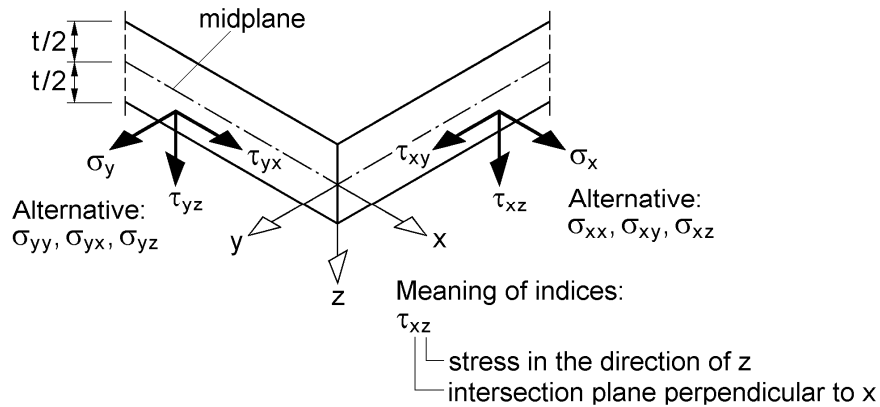
Figure 10.2   Stresses of plane load bearing structures

Plates with in-plane loading

The stresses of plates loaded in-plane shown in Figure 10.1 are summarised to resultant longitudinal and shear forces per unit length. Figure 10.3 contains the corresponding definitions according to DIN 1080 Part 2. In addition to the general procedure, the commonly used constant stress distributions and the longitudinal and shear forces resulting from these are shown on the right side of the figure. Because it is $\tau_{xy} = \tau_{yx}$, it is also $n_{xy} = n_{yx}$. The internal forces are forces per unit length and therefore they are designated with the **small** letter n. n_x and n_y are comparable to the axial force N of a beam member and n_{xy} to a shear force V.
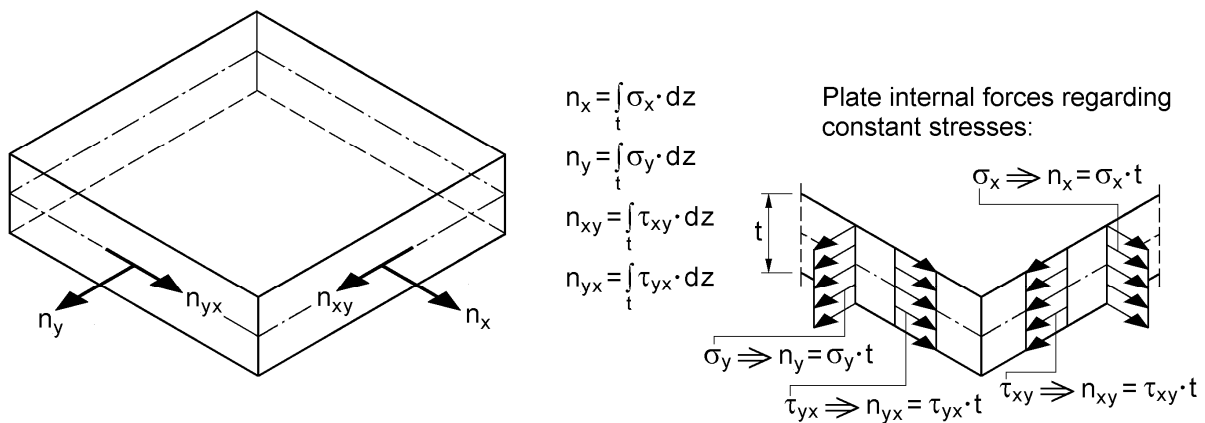
Figure 10.3   Longitudinal and shear forces of plates loaded in-plane

Plates with lateral loading

The internal forces of laterally loaded plates are also designated with a small letter since they are forces or moments per unit length (kN/m or kNm/m). Figure 10.4 shows the definition of the designations and the directions. However, in DIN 1080 Part 2, two different definitions are included. Selected and depicted here is the "orientation according to coordinates". In many publications and computer programs, the "orientation according to a characterised side" is used. With regard to stiffened plates, i. e. the combination of plates and beams, the designations in Figure 10.4 are more

advantageous. m_{xy} is comparable to the bending moment M_y for beams and m_{xx} to the torsional moment M_x. In addition to DIN 1080 Part 2, the stress distributions resulting from the internal plate forces according to the theory of elasticity are sketched in Figure 10.4 on the right side.

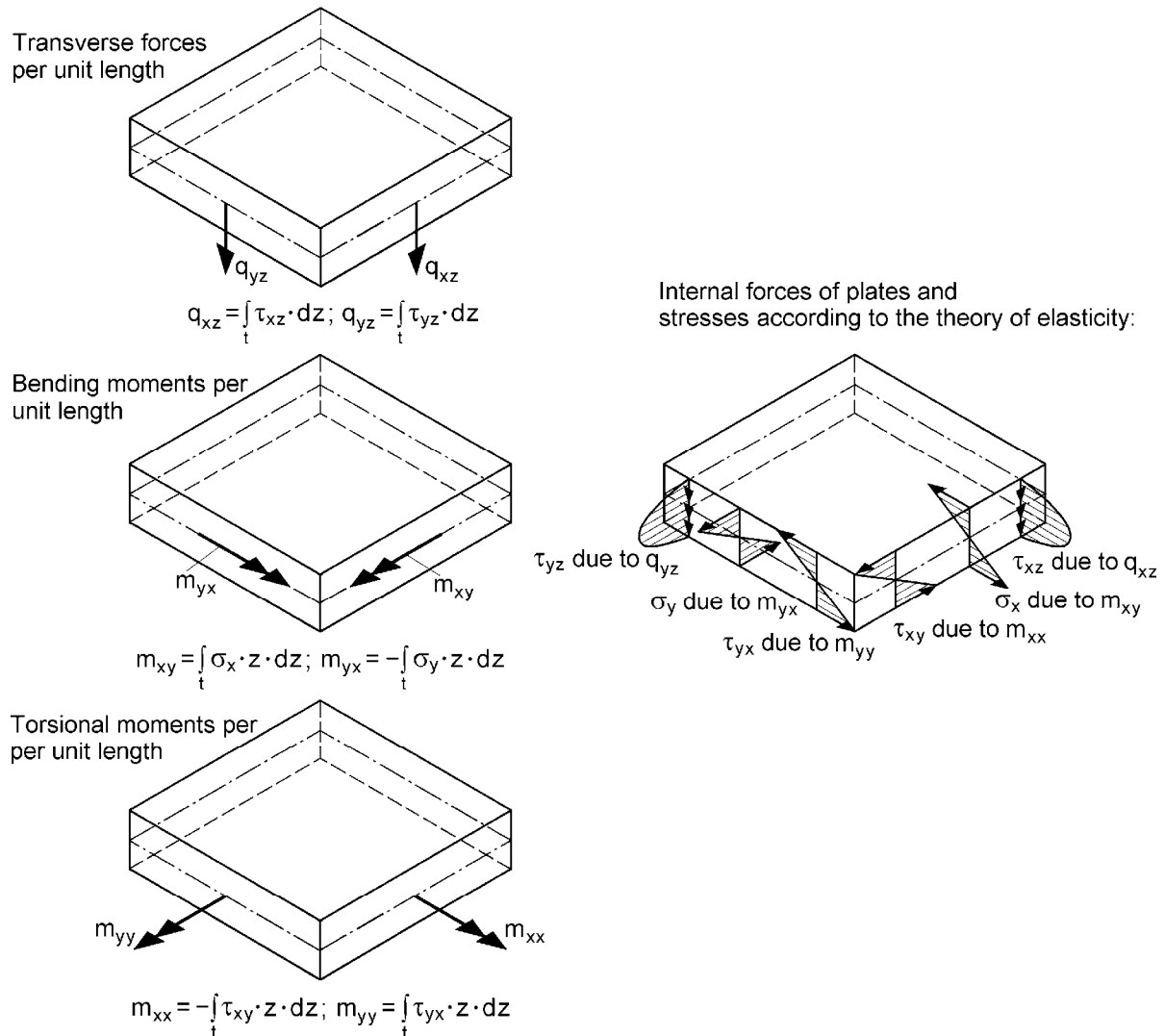**Figure 10.4**   Shear forces, bending moments and torsional moments of laterally loaded plates as well as stress distributions according to the theory of elasticity

10.3   Displacement Values

According to Figure 1.6, seven displacement values are distinguished for beams:

- Displacements u, v and w
- Rotations φ_x, φ_y and φ_z (or ϑ, w', v')
- Twist of the x-axis $\psi \cong \vartheta'$

In Figure 10.5, these displacement values are assigned to plates with lateral and in-plane loading and they are complemented with regard to the theory of plates. As already discussed in detail in Chapter 3.5.4, rectangular finite **plate** elements with four nodes and the nodal displacement values $w, w', w^{\bullet}$ and $w'^{\bullet}$ are recommended according to Figure 3.12. The displacement w describes the deflexion of the plate and the derivations w' and $w^{\bullet}$ are the corresponding rotations about the y- or x-axis, respectively. The following connection to the displacement values of beams is valid: $\varphi_y \triangleq -w'$ and $w^{\bullet} \triangleq \vartheta = \varphi_x$.

Additionally, $w'^{\bullet}$ is included, which is the derivation of the deflexion function w according to x and y. It corresponds to the twist ϑ' of beams. Due to $w'^{\bullet} = w^{\bullet'}$, it is also equal to $-\varphi_y^{\bullet}$, i.e. the change of the rotation φ_y in y-direction.

Plates with lateral loading:

$-w' \triangleq \varphi_y$ $w^{\bullet} \triangleq \vartheta = \varphi_x$

w

in addition: $w'^{\bullet} \triangleq \vartheta' = -\varphi_y^{\bullet}$

Plates with in−plane loading:

φ_z and $u^{\bullet}, v'$

v   u

$\varepsilon_{yx} \cong dv/dx$
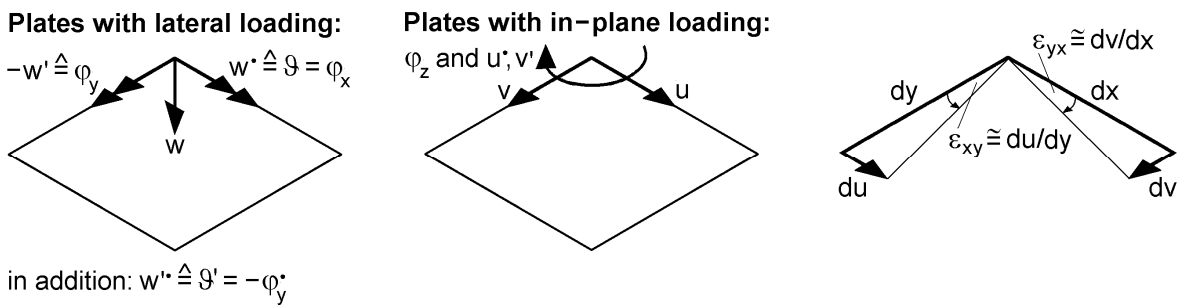
dy   dx

$\varepsilon_{xy} \cong du/dy$

du   dv

Figure 10.5   Displacement values for plates loaded laterally and in-plane

The deformations of plates loaded in-plane are described by displacement functions u(x,y) and v(x,y). Besides these displacements, the rotations $u^{\bullet} = \partial u / \partial y$ and $v' = \partial v / \partial x$ are used. Generally, they correspond to a rotation φ_z, for which, however, both components have to be distinguished due to the theory of plates. As for beams, the sum of the two angles leads to the shearing strain:

$$\gamma_{xy} = \frac{\partial u}{\partial y} + \frac{\partial v}{\partial x} = \varepsilon_{xy} + \varepsilon_{yx}. \tag{10.1}$$

The sketch in Figure 10.5 gives a corresponding illustration of that.

10.4 Constitutive Relationships

In Chapter 10.5, the virtual work for plates with lateral and in-plane loading is formulated. Just as for beams, some basic relationships are needed for that purpose, these are compiled below.

Hooke's **law for the plane stress state**

The assumption $\sigma_z = 0$ leads to the following strains and stresses:

$$\varepsilon_x = \frac{1}{E}\left(\sigma_x - \mu \cdot \sigma_y\right) \tag{10.2}$$

$$\varepsilon_y = \frac{1}{E}\left(\sigma_y - \mu \cdot \sigma_x\right) \tag{10.3}$$

$$\varepsilon_{xy} = \frac{1}{2G} \cdot \tau_{xy} \tag{10.4}$$

$$\sigma_x = \frac{E}{1-\mu^2}\left(\varepsilon_x + \mu \cdot \varepsilon_y\right) \tag{10.5}$$

$$\sigma_y = \frac{E}{1-\mu^2}\left(\varepsilon_y + \mu \cdot \varepsilon_x\right) \tag{10.6}$$

$$\tau_{xy} = \frac{E}{1+\mu} \cdot \varepsilon_{xy} \tag{10.7}$$

The following correlation exists for the material constants:

$$E = 2 \cdot (1 + \mu) \cdot G \tag{10.8}$$

Description of the displacement state

According to Chapter 1.6, the displacements u, v and w of beams are described by the deformations of the beam axes through the centre of gravity S and the shear centre M. Since the "centre of gravity line" and the "shear centre line" of plane structures are located in the centre face (S = M), for plates it is referred to this face. If the subscript "m" is used for labeling for **plates loaded in-plane** it is:

$$u = u_m \tag{10.9}$$

$$v = v_m \tag{10.10}$$

For **laterally loaded plates**, this is valid in a similar manner as for beams:

$$u = u_m + z \cdot \varphi_y \cong u_m - z \cdot w' \tag{10.11}$$

$$v = v_m - z \cdot \varphi_x \cong v_m - z \cdot w^{\bullet} \tag{10.12}$$

$$w = w_m \tag{10.13}$$

These correlations can directly be taken from Eq. (1.1) to (1.3), since at this point only the dependency of z is to be considered. The Eq. (10.11) to (10.13) are the starting point for *Kirchhoff's* plate theory, i. e. for plates with infinite shear stiffness.

Relationships between strains and displacement values

According to [25] and many other publications, the following formulas are valid for the linear theory, i. e. for small deformations:

$$\varepsilon_x = u' \tag{10.14}$$

$$\varepsilon_y = v^\bullet \tag{10.15}$$

$$\varepsilon_{xy} = \varepsilon_{yx} = 1/2 \cdot \left(u^\bullet + v' \right) \tag{10.16}$$

With regard to the buckling of plates, the geometric nonlinearity has to in addition be considered in terms of the second order theory. If one proceeds as shown in Chapter 5.3 for beams and the result of Eq. (5.29) is transferred to plates, one obtains:

$$\varepsilon_x = u' + 1/2 \cdot \left(w' \right)^2 \tag{10.17}$$

$$\varepsilon_y = v^\bullet + 1/2 \cdot \left(w^\bullet \right)^2 \tag{10.18}$$

$$\varepsilon_{xy} = 1/2 \cdot \left(u^\bullet + v' \right) + 1/2 \cdot w' \cdot w^\bullet \tag{10.19}$$

Using Eq. (10.11) to (10.13), it can be referred to the displacements of the centre face and the following relationships result for the strains:

$$\varepsilon_x = u'_m - z \cdot w''_m + 1/2 \cdot \left(w'_m \right)^2 \tag{10.20}$$

$$\varepsilon_y = v^\bullet_m - z \cdot w^{\bullet\bullet}_m + 1/2 \cdot \left(w^\bullet_m \right)^2 \tag{10.21}$$

$$\varepsilon_{xy} = 1/2 \cdot \left(u^\bullet_m - z \cdot w'^\bullet + v'_m - z \cdot w'^\bullet + w'_m \cdot w^\bullet_m \right) \tag{10.22}$$

10.5 Principle of the Virtual Work

Just as for beams, the following equation is also used for *plane load bearing structures* as equilibrium condition:

$$\delta W = \delta W_{ext} + \delta W_{int} = 0 \tag{10.23}$$

Explanations on the virtual work can be found in Chapter 3.4.2.

Internal virtual work

According to [25], the following is generally valid:

$$\delta W_{int} = -\int_V \delta \underline{\varepsilon} \cdot \underline{\sigma} \cdot dV \tag{10.24}$$

For *plane structures*, the volume integral can be formulated as follows:

$$\delta W_{int} = -\int_A \int_{-t/2}^{+t/2} \left(\delta \varepsilon_x \cdot \sigma_x + \delta \varepsilon_y \cdot \sigma_y + \delta \varepsilon_{xy} \cdot \tau_{xy} + \delta \varepsilon_{yx} \cdot \tau_{yx} \right) \cdot dz \cdot dA \tag{10.25}$$

As it is common practice, shear stresses τ_{xz} and τ_{yz}, i. e. perpendicular to the centre face, are neglected. In Eq. (10.25), the virtual strains can be replaced using Eq. (10.20) to (10.22) after formation of the variation. If the stresses are substituted using Eq. (10.5) to (10.7) and the Formulas (10.20) to (10.22), the virtual work is a function of the displacement functions $u_m(x,y)$, $v_m(x,y)$ and $w_m(x,y)$. Within the scope of the second order theory, **double** products of the displacement functions are considered at maximum. Since it is

$$\int_{-t/2}^{+t/2} z \cdot dz = 0 \tag{10.26}$$

one obtains the following work components:

a) Plates loaded in-plane

$$\delta W_{int} = -\int_A \Big[D \cdot \left(\delta u_m' \cdot u_m' + \delta u_m' \cdot \mu \cdot v_m^\bullet + \delta v_m^\bullet \cdot v_m^\bullet + \delta v_m^\bullet \cdot \mu \cdot u_m' \right)$$

$$+ G \cdot t \cdot \left(\delta u_m^\bullet \cdot u_m^\bullet + \delta u_m^\bullet \cdot v_m' + \delta v_m' \cdot u_m^\bullet + \delta v_m' \cdot v_m' \right) \Big] \cdot dA \tag{10.27}$$

b) Plates laterally loaded

$$\delta W_{int} = -\int_A \Big[B \cdot \left(\delta w_m'' \cdot w_m'' + \delta w_m'' \cdot \mu \cdot w_m^{\bullet\bullet} + \delta w_m^{\bullet\bullet} \cdot w_m^{\bullet\bullet} + \delta w_m^{\bullet\bullet} \cdot \mu \cdot w_m'' \right)$$

$$+ G \cdot t^3/12 \cdot \left(\delta w_m^{\bullet\prime} \cdot w_m^{\bullet\prime} + \delta w_m^{\bullet\prime} \cdot w_m^{\bullet\prime} + \delta w_m^{\bullet\prime} \cdot w_m^{\bullet\prime} + \delta w_m^{\bullet\prime} \cdot w_m^{\bullet\prime} \right) \Big] \cdot dA \tag{10.28}$$

c) Coupling in-plane/laterally loaded plates (for plate buckling)

$$\delta W_{int} = -\int_A \Big[\delta w_m' \cdot n_x \cdot w_m' + \delta w_m^\bullet \cdot n_y \cdot w_m^\bullet + n_{xy} \left(\delta w_m' \cdot w_m^\bullet + \delta w_m^\bullet \cdot w_m' \right) \Big] \cdot dA$$

$$\tag{10.29}$$

In Eq. (10.27), D is the *extensional stiffness of the plate* is

$$D = \frac{E \cdot t}{1 - \mu^2} \tag{10.30}$$

and in Eq. (10.28), B the *bending stiffness of the plate*:

$$B = \frac{E \cdot t^3}{12 \cdot \left(1 - \mu^2\right)}$$

(10.31)

Equation (10.29) contains the longitudinal and shear forces n_x, n_y and n_{xy} of the plates loaded in-plane according to Figure 10.3, i. e. the stresses σ_x, σ_y and τ_{xy}, which are linked to the plate deflexion $w_m(x,y)$. Since A is the centre face of the *plane structure*, for rectangular plates it is:

$$dA = dx \cdot dy$$

(10.32)

External virtual work

In Chapter 3.4.2, the formulation of the virtual work for beams is dealt with and Table 3.2 contains a compilation for concentrated loads and distributed loads. Using this, the external virtual work for plates can directly be stated. With the help of Figure 10.6, it is exemplarily formulated here for selected loads of plates:

$$\delta W_{ext} = F_z \cdot \delta w_{Fz} + \int_{x=a}^{x=b} q_z \cdot \delta w_{qz} \cdot dx$$

(10.33)

In Eq. (10.33), δw_{Fz} and δw_{qz} are the virtual displacements in the direction of acting loads. For a constant area load p_z, the integration is supposed to be formed via the loaded area, so that the external virtual work yields as follows:

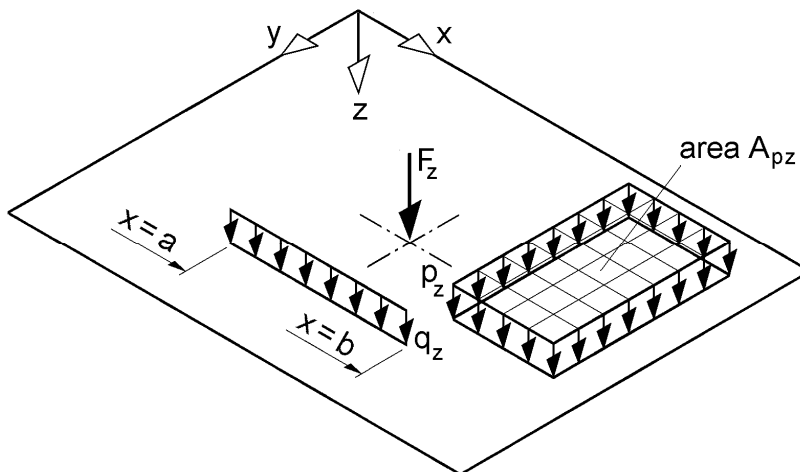$$\delta W_{ext} = \int_{A_{pz}} p_z \cdot \delta w_{pz} \cdot dA$$

(10.34)

Figure 10.6   Loads F_z, q_z and p_z for plates

10.6   Plates in Steel Structures

Usually, steel constructions are almost exclusively idealised as lattice structures. Regarding profile-oriented structures, which are often realised with rolled cross sections, this is in the nature of things, since they are actually beam-shaped constructions. Other structures which seem planar at first glance are also treated as *lattice structures* for the calculation of the deformations and stresses. Even large bridges are idealised using girders, girder grid constructions or spatial lattice structures and the engineering standards are adjusted to these calculations as well, this is for instance realised with the specification of an effective width of flanges.

If, by way of exception, plane load-bearing structures are consulted for the calculation, it may for example be a case of load introduction problems, which are calculatively analysed with the help of plates. Nevertheless, analyses with the FEM are rare since they are actually only suitable if the material fatigue is to be considered. Otherwise, i. e. if local plastifications can be accepted, one usually uses simplified design models as for instance for the load introduction into I-profiles without stiffeners as shown in Figure 10.7 for example.
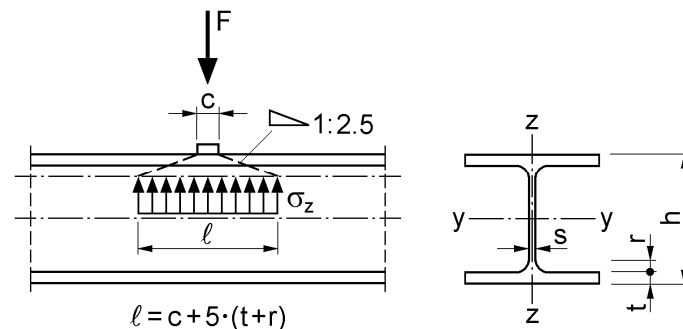

Figure 10.7   Design model for the transmission of force into I-sections without stiffeners

Another possible case for the use of plate elements for steel structures may be the analysis for the load-bearing capacity of beams with thin-walled cross sections. Figure 10.8 shows different cross sections for which the different parts are idealised using plates. However, for engineering practice, this application is of no relevance, it is only of interest for scientific analyses. Sporadically, this methodology has been used for the examination of bridges. Whether this is reasonable or not has not generally been clarified yet.
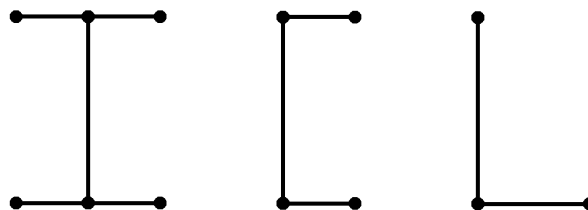

Figure 10.8   Idealisation of thin cross sectional parts through plates (plane shell)

A reasonable field of application for the use of plate elements is plate buckling, although the calculations are normally not executed with the FEM, but conducted by using formulas or tables. Usually, plate buckling is about the analysis of plane load-bearing structures being components of lattice structures. A typical example of that are bridges, where single or stiffened plates are extracted in order to analyse the influence of the buckling on the bearing capacity of the components. Figure 10.9 gives an explanatory example. Due to the significance of plate buckling for steel structures, it is discussed in the following Chapters in detail and initially the basics for the application of the FEM are derived.
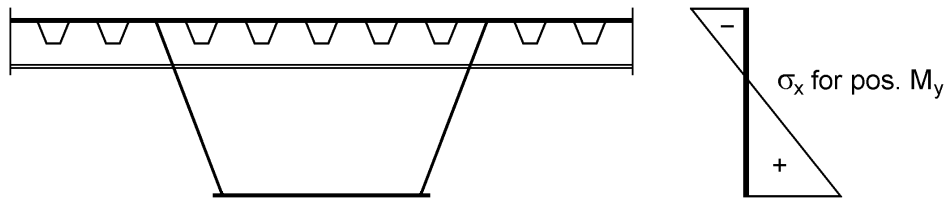
- Upper flange: Field range of single-span and continuous beams (pos. M_y)
- Webs: End-bearing (shear force), field range (pos. M_y), supported areas of continuous beams (neg. M_y and shear force)
- Lower flange: Supported areas of continuous beams (neg. M_y)

Figure 10.9   Required verifications against plate buckling using the example of a pedestrian bridge

10.7   Stiffness Matrix for a Plate Element

In this Chapter, the stiffness matrix for a plate element with infinite shear stiffness is derived on the basis of *Kirchhoff's* plate theory. As explained in detail in Chapter 3.5.4, a rectangular plate element with four nodes and a total of 16 nodal degrees of freedom is chosen. At each node, w, w', $w^{\bullet}$ and $w'^{\bullet}$ are the unknown displacement values.

The bicubic polynomial function chosen with the help of Figure 3.14 leads to the following displacement function for the deflexion of the plate element in Figure 3.16:

$$
\begin{aligned}
w(x,y) = {} & c_1 + c_2 \cdot x + c_3 \cdot y + c_4 \cdot x^2 + c_5 \cdot xy + c_6 \cdot y^2 + c_7 \cdot x^3 + c_8 \cdot x^2 y \\
& + c_9 \cdot xy^2 + c_{10} \cdot y^3 + c_{11} \cdot xy^3 + c_{12} \cdot x^3 y + c_{13} \cdot x^2 y^2 \\
& + c_{14} \cdot x^2 y^3 + c_{15} \cdot x^3 y^2 + c_{16} \cdot x^3 y^3
\end{aligned}
\tag{10.35}
$$

Similar to beams, the dimensionless coordinates $\xi = x/\ell_x$ and $\eta = y/\ell_y$ are introduced and the unknowns c_1 to c_{16} are replaced by the unknown displacement values at the four nodes:

w_a, w_a', $w_a^{\bullet}$, $w_a^{\prime\bullet}$, w_b, w_b', $w_b^{\bullet}$, $w_b^{\prime\bullet}$, w_c, w_c', $w_c^{\bullet}$, $w_c^{\prime\bullet}$, w_d, w_d', $w_d^{\bullet}$ and $w_d^{\prime\bullet}$.

As a result, one obtains the displacement function $w(\xi,\eta)$ in the formulation of Eq. (3.58), see also Figure 3.10. The subscript "m" for the designation of the plate centre face is omitted here for reasons of a simplified depiction and a better readability.
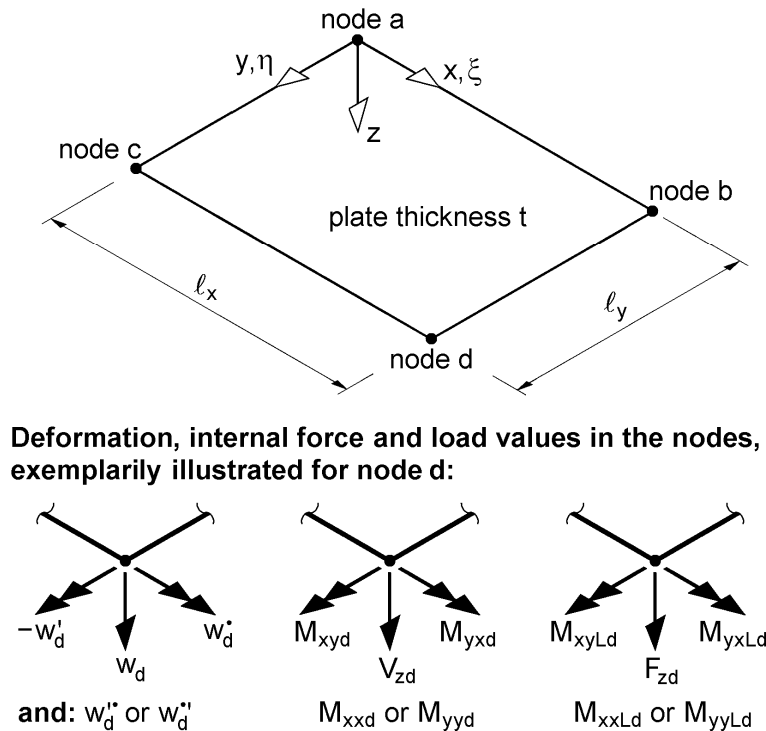
Figure 10.10 Rectangular plate element with 16 degrees of freedom and deformation, internal and load values in the nodes

In Figure 10.10, the rectangular plate element with the chosen designations is represented. The internal forces and loads correspond to the four deformation values at the nodes. They are values in kN or kNm, respectively, and are therefore designated with **capital** letters. The indices comply with the definitions of Figure 10.4 for the internal forces of the plate. The subscript "L" designates the load values, as shown in Figure 1.4 for beams.

The stiffness relationship for the plate element in Figure 10.10 can now be formulated in a similar manner as it was shown in Chapter 4.2 for beam elements. In doing so, especially the comparison with Eq. (4.18) and Table 4.2 directly leads to the desired result. For the plate element, the stiffness relation is:

$$
\begin{array}{l}
\delta w_a : \\
-\delta w_a' \cdot \ell_x : \\
\delta w_a^\bullet \cdot \ell_y : \\
\delta w_a'^\bullet \cdot \ell_x \cdot \ell_y : \\
\delta w_b : \\
-\delta w_b' \cdot \ell_x : \\
\delta w_b^\bullet \cdot \ell_y : \\
\delta w_b'^\bullet \cdot \ell_x \cdot \ell_y : \\
\delta w_c : \\
-\delta w_c' \cdot \ell_x : \\
\delta w_c^\bullet \cdot \ell_y : \\
\delta w_c'^\bullet \cdot \ell_x \cdot \ell_y : \\
\delta w_d : \\
-\delta w_d' \cdot \ell_x : \\
\delta w_d^\bullet \cdot \ell_y : \\
\delta w_d'^\bullet \cdot \ell_x \cdot \ell_y :
\end{array}
\begin{bmatrix}
V_{za} \\
M_{xya} \\
M_{yxa} \\
M_{xxa} \\
V_{zb} \\
M_{xyb} \\
M_{yxb} \\
M_{xxb} \\
V_{zc} \\
M_{xyc} \\
M_{yxc} \\
M_{xxc} \\
V_{zd} \\
M_{xyd} \\
M_{yxd} \\
M_{xxd}
\end{bmatrix}
=
\begin{bmatrix}
\text{16}\times\text{16 element} \\
\text{stiffness matrix,} \\
\text{see Table 10.1}
\end{bmatrix}
\cdot
\begin{bmatrix}
w_a \\
-w_a' \cdot \ell_x \\
w_a^\bullet \cdot \ell_y \\
w_a'^\bullet \cdot \ell_x \cdot \ell_y \\
w_b \\
-w_b' \cdot \ell_x \\
w_b^\bullet \cdot \ell_y \\
w_b'^\bullet \cdot \ell_x \cdot \ell_y \\
w_c \\
-w_c' \cdot \ell_x \\
w_c^\bullet \cdot \ell_y \\
w_c'^\bullet \cdot \ell_x \cdot \ell_y \\
w_d \\
-w_d' \cdot \ell_x \\
w_d^\bullet \cdot \ell_y \\
w_d'^\bullet \cdot \ell_x \cdot \ell_y
\end{bmatrix}
-
\begin{bmatrix}
F_{za} \\
M_{xyLa} \\
M_{yxLa} \\
M_{xxLa} \\
F_{zb} \\
M_{xyLb} \\
M_{yxLb} \\
M_{xxLb} \\
F_{zc} \\
M_{xyLc} \\
M_{yxLc} \\
M_{xxLc} \\
F_{zd} \\
M_{xyLd} \\
M_{yxLd} \\
M_{xxLd}
\end{bmatrix}
$$

$$
\delta \underline{v}_e^T : \qquad \underline{s}_e \;=\; \underline{K}_e \;\cdot\; \underline{v}_e \;-\; \underline{p}_e \qquad (10.36)
$$

The element stiffness matrix $\underline{K}_e$ for the bending of plates can be stated explicitly with the virtual work in Eq. (10.28), if one uses the displacement function $w(\xi,\eta)$ according to Eq. (3.58) for the deflexion of the plate. To do so, the relevant derivations of the function have to be set up and the integration over the plate area has to be performed. Since the displacement function in Eq. (3.58) is formulated with dimensionless coordinates, $dA = dx \cdot dy$ is replaced by $d\xi \cdot d\eta \cdot \ell_x \cdot \ell_y$ in Eq. (10.28) and the integration is executed from $\xi = 0$ to $\xi = 1$ as well as $\eta = 0$ to $\eta = 1$. The result is the stiffness matrix stated in Table 10.1 for the plate element of Figure 10.10. Each component of the matrix consists of four terms which are to be added after the multiplication with the given factors. The shear modulus G in Eq. (10.28) was replaced by the material constants E and μ with the help of Formula (10.8). In Eq. (10.36), the vectors $\delta \underline{v}_e^T$ and $\underline{v}_e$ contain the element lengths ℓ_x and ℓ_y. These lengths have to be multiplied into the element stiffness matrix of Table 10.1 if plates are supposed to be discretised using elements of different lengths.

Table 10.1　　Stiffness matrix for the plate element in Figure 10.10

	1	2	3	4	5	6	7	8	9	10	11	12	13	14	15	16
1	2808	1404	396	198	972	486	-234	-117	-2808	1404	-396	198	-972	486	234	-117
	2808	396	1404	198	-2808	-396	1404	198	972	-234	486	-117	-972	234	486	-117
	1296	648	648	99	-1296	-648	108	54	-1296	108	-648	54	1296	-108	-108	9
	1296	108	108	9	-1296	-108	108	9	-1296	108	-108	9	1296	-108	-108	9
2		936	198	132	486	324	-117	-78	-1404	468	-198	66	-486	162	117	-39
		72	198	36	-396	-72	198	36	234	-54	117	-27	-234	54	117	-27
		144	549	72	-648	-144	54	12	-108	-36	-54	-18	108	36	-9	-3
		144	9	12	-108	-144	9	12	-108	-36	-9	-3	108	36	-9	-3
3			72	36	234	117	-54	-27	-396	198	-72	36	-234	117	54	-27
			936	132	-1404	-198	468	66	486	-117	324	-78	-486	117	162	-39
			144	72	-108	-54	-36	-18	-648	54	-144	12	108	-9	36	-3
			144	12	-108	-9	-36	-3	-108	9	-144	12	108	-9	36	-3
4				24	117	78	-27	-18	-198	66	-36	12	-117	39	27	-9
				24	-198	-36	66	12	117	-27	78	-18	-117	27	39	-9
				16	-54	-12	-18	-4	-54	-18	-12	-4	9	3	3	1
				16	-9	-12	-3	-4	-9	-12	-4	-4	9	3	3	1
5					2808	1404	-396	-198	-972	486	-234	117	-2808	1404	396	-198
					2808	396	-1404	-198	-972	234	-486	117	972	-234	-486	117
					1296	648	-648	-99	1296	-108	108	-9	-1296	108	648	-54
					1296	108	-108	-9	1296	-108	108	-9	-1296	108	108	-9
6						936	-198	-132	-486	162	-117	39	-1404	468	198	-66
						72	-198	-36	-234	54	-117	27	234	-54	-117	27
						144	-549	-72	108	36	9	3	-108	-36	54	18
						144	-9	-12	108	36	9	3	-108	-36	9	3
7							72	36	234	-117	54	-27	396	-198	-72	36
							936	132	486	-117	162	-39	-486	117	324	-78
							144	72	-108	9	36	-3	648	-54	-144	12
							144	12	-108	9	36	-3	108	-9	-144	12
8								24	117	-39	27	-9	198	-66	-36	12
								24	117	-27	39	-9	-117	27	78	-18
								16	-9	-3	3	1	54	18	-12	-4
								16	-9	-3	3	1	9	3	-12	-4
9									2808	-1404	396	-198	972	-486	-234	117
									2808	-396	1404	-198	-2808	396	1404	-198
									1296	-648	648	-99	-1296	648	108	-54
									1296	-108	108	-9	-1296	108	108	-9
10										936	-198	132	-486	324	117	-78
										72	-198	36	396	-72	-198	36
										144	-549	72	648	-144	-54	12
										144	-9	12	108	-144	-9	12
11											72	-36	234	-117	-54	27
											936	-132	-1404	198	468	-66
											144	-72	-108	54	-36	18
											144	-12	-108	9	-36	3
12												24	-117	78	27	-18
												24	198	-36	-66	12
												16	54	-12	18	-4
												16	9	-12	3	-4
13													2808	-1404	-396	198
													2808	-396	-1404	198
													1296	-648	-648	99
													1296	-108	-108	9
14														936	198	-132
														72	198	-36
														144	549	-72
														144	9	-12
15															72	-36
															936	-132
															144	-72
															144	-12
16																24
																24
																16
																16

Matrix is symmetric.

Factors for the 4 values of the matrix elements:

- $\dfrac{B \cdot \ell_y}{630 \cdot \ell_x^3}$

- $\dfrac{B \cdot \ell_x}{630 \cdot \ell_y^3}$

- $\dfrac{\mu \cdot B}{450 \cdot \ell_x \cdot \ell_y}$

- $\dfrac{(1-\mu) \cdot B}{450 \cdot \ell_x \cdot \ell_y}$

$$\text{mit}: B = \frac{E \cdot t^3}{12 \cdot (1-\mu^2)}$$

σ_x and σ_y as positive tensile stresses.

10.8　Geometric Stiffness Matrix for Plate Buckling

Following, the stiffness relationship for the bending of plates according to Eq. (10.36) is expanded for the analysis of plate buckling. For this purpose, a geometric element

stiffness matrix $\underline{G}_e$ is added to the stiffness relationship as done in Chapter 5.5 for beams:

$$\hat{\underline{s}}_e = \left(\underline{K}_e + \underline{G}_e\right) \cdot \underline{v}_e - \underline{p}_e \tag{10.37}$$

The differentiation of the internal forces $\underline{s}_e$ and $\hat{\underline{s}}_e$ (see Figure 5.9) is not explicitly required here and the vector of the load $\underline{p}_e$ is not needed since only the eigenvalue problem "plate buckling" is supposed to be solved.

Table 10.2   Geometric stiffness matrix for the plate element in Figure 10.10

	1	2	3	4	5	6	7	8	9	10	11	12	13	14	15	16
1	5616 / 5616 / 900	468 / 792 / 0	792 / 468 / 0	66 / 66 / -36	1944 / -5616 / 0	162 / 66 / -180	-468 / 468 / 0	-39 / 66 / 36	-5616 / 1944 / 0	468 / -468 / 0	-792 / 162 / -180	66 / -39 / 36	-1944 / -1944 / -900	162 / 468 / 180	468 / 162 / 180	-39 / -39 / -36
2		624 / 144 / 0	66 / 66 / 36	88 / 12 / 0	162 / -792 / 180	216 / -144 / 0	-39 / 66 / -36	-52 / 12 / 0	-468 / 468 / 0	-156 / -108 / 0	-66 / 39 / -36	-22 / -9 / 6	-162 / -468 / -180	-54 / 108 / 30	39 / 39 / 36	13 / -9 / -6
3			144 / 624 / 0	12 / 88 / 0	468 / -468 / 0	39 / -66 / -36	-108 / -156 / 0	-9 / -22 / 6	-792 / 162 / 180	66 / -39 / -36	-144 / 216 / 0	12 / -52 / 0	-468 / -162 / -180	39 / 39 / 36	108 / -54 / 30	-9 / 13 / -6
4				16 / 16 / 0	39 / -66 / 36	52 / -12 / 0	-9 / -22 / -6	-12 / -4 / 0	-66 / 39 / 36	-22 / -9 / -6	-12 / 52 / 0	-4 / -12 / 0	-39 / -39 / -36	-13 / 9 / 6	9 / -13 / 6	3 / 3 / -1
5					5616 / 5616 / -900	468 / 792 / 0	-792 / -468 / 0	-66 / -66 / -36	-1944 / -1944 / 900	162 / 468 / -180	-468 / -162 / 180	39 / 39 / -36	-5616 / 1944 / 0	468 / -468 / 0	792 / -162 / -180	-66 / 39 / 36
6						624 / 144 / 0	-66 / -66 / 36	-88 / -12 / 0	-162 / -468 / 180	-54 / 108 / -30	-39 / -39 / 36	-13 / 9 / -6	-468 / 468 / 0	-156 / -108 / 0	66 / -39 / -36	22 / 9 / 6
7							144 / 624 / 0	12 / 88 / 0	468 / 162 / -180	-39 / -39 / 36	108 / -54 / -30	-9 / 13 / 6	792 / -162 / 180	-66 / 39 / -36	-144 / 216 / 0	12 / -52 / 0
8								16 / 16 / 0	39 / 39 / -36	13 / -9 / 6	9 / -13 / -6	3 / 3 / 1	66 / -39 / 36	22 / 9 / -6	-12 / 52 / 0	-4 / -12 / 0
9									5616 / 5616 / -900	-468 / -792 / 0	792 / 468 / 0	-66 / -66 / -36	1944 / -5616 / 0	-162 / 792 / -180	-468 / 468 / 0	39 / -66 / 36
10										624 / 144 / 0	-66 / -66 / 36	88 / 12 / 0	-162 / 792 / 180	216 / -144 / 0	39 / -66 / -36	-52 / 12 / 0
11											144 / 624 / 0	-12 / -88 / 0	468 / -468 / 0	-39 / 66 / -36	-108 / -156 / 0	9 / 22 / 6
12												16 / 16 / 0	-39 / 66 / 36	52 / -12 / 0	9 / 22 / -6	-12 / -4 / 0
13													5616 / 5616 / 900	-468 / -792 / 0	-792 / -468 / 0	66 / 66 / -36
14														624 / 144 / 0	66 / 66 / 36	-88 / -12 / 0
15															144 / 624 / 0	-12 / -88 / 0
16																16 / 16 / 0

Matrix is symmetric.

Factors for the 3 values of the matrix elements:

- $\dfrac{\sigma_x \cdot t \cdot \ell_y}{12600 \cdot \ell_x}$
- $\dfrac{\sigma_y \cdot t \cdot \ell_x}{12600 \cdot \ell_y}$
- $\dfrac{\tau_{xy} \cdot t}{1800}$

The starting point for the setup of the matrix $\underline{G}_e$ is the virtual work in Eq. (10.29). As for the lateral buckling of beam members, the internal forces $n_x = \sigma_x \cdot t$, $n_y = \sigma_y \cdot t$ and $n_{xy} = \tau_{xy} \cdot t$ are assumed to be known. Moreover, it is assumed that they are **constant** within the element. In a similar manner as described in Chapter 10.7 for the plate bending, the necessary integrations can be carried out without any problems. The geometric element stiffness matrix shown in Table 10.2 is the result. Each element of

the matrix consists of three terms which are to be added after the multiplication with the given factors.

As an alternative to the assumption of **constant** in-plane internal forces within the plate elements also **linearly or quadratically nonuniform courses** can be regarded. The integrations are somewhat more extensive then and the geometric stiffness matrix is significantly more complex since the matrix elements have two or three times as many terms.

10.9 Longitudinally and Laterally Stiffened Plates

Plates are often strengthened in longitudinal and lateral direction. The stiffened plates can be analysed with a combination of plate and beam elements using the FEM.
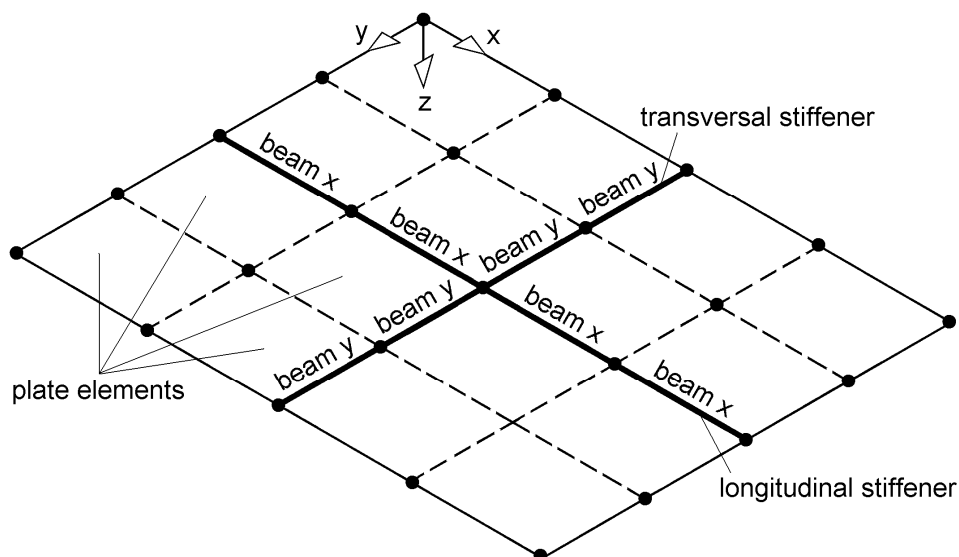
Figure 10.11 Plate with a longitudinal and a transversal stiffener

The plate of Figure 10.11, which is supposed to represent a partition of a larger plate, is stiffened with a longitudinal and a transversal stiffener. It is divided into finite plate elements, which also directly leads to the corresponding beam elements. For the setup of the stiffness matrix $\underline{K}$ and the geometric stiffness matrix $\underline{G}$, first the plate elements are considered. The allocation of the matrix elements is carried out as described in Chapter 4.5.2 for lattice structures. In a second step, the beam elements are added. For **beams in x-direction**, the element stiffness matrices can directly be taken from Chapters 4.2.3, 4.2.4 and 5.6. Since the bending about the y-axis and the warping torsion are to be acquired, 8×8 element matrices ensue. The allocation of the degrees of freedom of the beams to the ones of the plates is also possible without any problems. With the assumption that the beam element begins at the point a and ends at point b, the following allocation results with Figures 4.2 and 10.12:

$$w_{Ma} \rightarrow w_a$$

$$\varphi_{ya} \rightarrow -w_a'$$

$$\vartheta_a \rightarrow w_a^{\bullet}$$

$$-\vartheta_a' \rightarrow w_a'^{\bullet}$$

$$w_{Mb} \rightarrow w_b$$

$$\varphi_{yb} \rightarrow -w_b'$$

$$\vartheta_b \rightarrow w_b^{\bullet}$$

$$-\vartheta_b' \rightarrow w_b'^{\bullet}$$
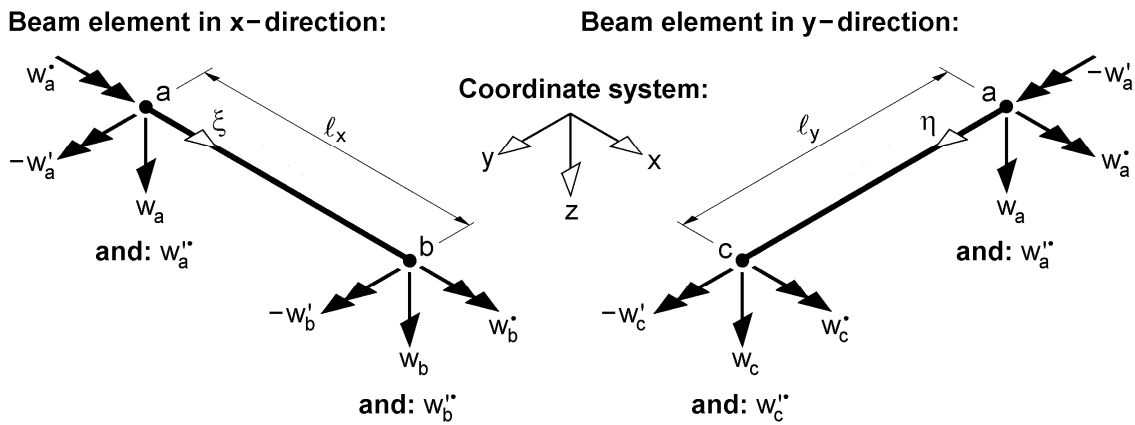
**Figure 10.12** Beam elements in x and y-direction and allocation of the degrees of freedom to the plates

The necessary matrices for the beam elements can be set up using Tables 4.3 and 5.2. However, only matrix elements are to be adopted which are linked to the deformations mentioned previously. According to Table 4.3, these elements of the stiffness matrix are the ones depending on the stiffnesses EI_y, EI_ω and GI_T. The values to be taken from the geometric element stiffness matrix (see Table 5.2) depend on the particular task. As a general rule, only xial forces N are considered in the stiffeners for plate buckling and therefore the components depending on N, which are linked to the deformation values stated above, need to be regarded. In doing so, it has to be noted that M_{rr} is influenced by the axial force N, see Table 5.1. An additional look into Table 4.3 shows that distributed springs c_w and c_ϑ can also be considered for plate buckling.

For **beam elements in y-direction**, which run from a to c, the allocation of the degrees of freedom can be also carried out with Figures 4.2 and 10.12. The selection of the matrix elements is done similarly as for beam elements in x-direction.

FEM for stiffened buckling plates

Figure 10.13 exemplarily shows a buckling plate which is stiffened by a longitudinal stiffener and stressed by constantly distributed stresses σ_x only.
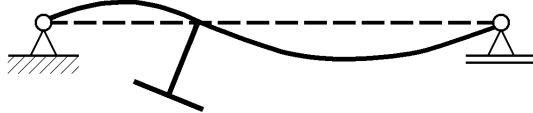
a) Stiffened buckling panel
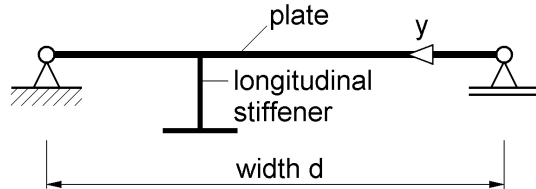
b) FE-modelling
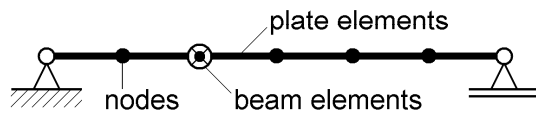
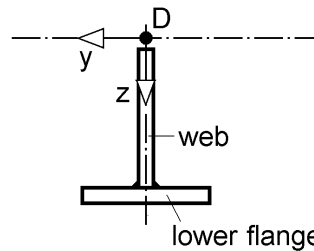c) Buckling of the single panel

d) Buckling of the entire panel
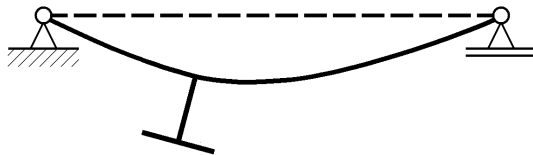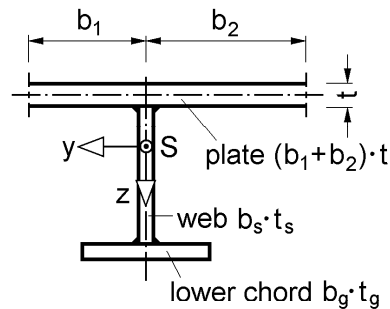
Figure 10.13 Buckling plate with a longitudinal stiffener and
cross section properties of the stiffener

According to Figure 10.13a, the stress σ_x is set to be constant over the total height since the buckling plates are usually components of total cross sections. For the FE-modelling, the **plate** is laterally and longitudinally divided into finite plate elements, providing a bending stiffness and being stressed by "in-plane stresses".

Figure 10.13b exemplarily shows six equal elements in lateral direction. **Stiffeners** are usually arranged on one side regarding the plate centre face, which is also the case for the T-stiffener in Figure 10.13. It is idealised using beam elements, for which the stiffnesses EI_y, GI_T and EI_ω as well as, with respect to the stability risk, the compression force $N = \sigma_x \cdot A$ and $N \cdot i_p^2$ are required. The values are to be calculated as follows:

- **Moment of inertia I_y (bending)**

  The stiffened plate acts as upper flange of the stiffener. Therefore, I_y is to be calculated considering the effective flange width $b_1 + b_2$, also see Figure 10.18 and Table 10.3. Since the bending of the plate is already included in the stiffness matrix (see Table 10.1), the upper flange may only be considered with the *Steiner*-part for the I_y of the stiffener.

- **Torsion constant I_T (primary torsion)**

  For this value only the stiffener itself may be considered since the corresponding stiffness of the plate is already included in the stiffness matrix (see Table 10.1). This becomes obvious with the virtual work of Eq. (10.28) and the term depending on the shear modulus G. For thin-walled stiffeners (open cross section!) it is:

$$I_T = \frac{1}{3} b_s \cdot t_s^3 + \frac{1}{3} b_g \cdot t_g^3 \tag{10.38}$$

- **Warping constant I_ω (secondary torsion)**

  For the calculation of this value, the pivot point is assumed to be in the centre face of the plate since the plate cannot displace laterally. With this assumption, the warping ordinate for the edges of the lower flange of the stiffener is

$$\omega_g = \pm \left(t/2 + b_s + t_g/2 \right) \cdot b_g/2 \quad \text{and the warping constant is} \tag{10.39}$$

$$I_\omega = \int_A \omega^2 \cdot dA = \frac{1}{3} \omega_g^2 \cdot b_g \cdot t_g \tag{10.40}$$

- **Compression force N for lateral buckling**

  For the lateral buckling of the stiffener the axial force $N = \sigma_x \cdot A$ is of importance. A is the cross section area of the stiffener, i. e. here in this case it is $A = b_s \cdot t_s + b_g \cdot t_g$. Parts of the plate are not regarded since the compression stresses σ_x are already included in the geometric stiffness matrix (see Table 10.2).

- **$N \cdot i_p^2$ for torsional buckling**

  For the torsional buckling of the stiffener, the origin of the rotation is assumed in the centre face of the plate as done for the warping constant I_ω. For M_{rr} of Tables 5.1 and 5.2 with $\sigma_x = $ const., it is therefore:

$$M_{rr} = \int_A \sigma_x \cdot \left(y^2 + z^2 \right) \cdot dA = \sigma_x \cdot \int_A \left(y^2 + z^2 \right) \cdot dA$$

$$= \sigma_x \cdot \left(I_z + I_y \right) = \sigma_x \cdot I_p = \sigma_x \cdot A \cdot i_p^2 \tag{10.41}$$

For the stiffener in Figure 10.13, one obtains

$$I_z = t_g \cdot b_g^3 / 12 \tag{10.42}$$

$$I_y = t_s \cdot b_s^3 / 12 + t_s \cdot b_s \cdot \left(t/2 + b_s/2 \right)^2 + t_g \cdot b_g \cdot \left(t/2 + b_s + t_g/2 \right)^2 \tag{10.43}$$

For hand calculations, the torsional stiffnesses GI_T and EI_ω of stiffeners are usually neglected and a "minimum torsional buckling stiffness" is demanded for compressed stiffeners with an open cross section shape. Specifications on this are given in DIN 18800 Part 3 for instance, an example would be element 1004. Often, FE-calculations are also conducted for $EI_\omega = GI_T = 0$. If these stiffnesses are considered, which is possible without any difficulty, the danger of torsional buckling of the stiffener has to be captured with $N \cdot i_p^2$ in the geometric stiffness matrices of the beam elements.

With the eigenvalue analysis of the plate buckling of Figure 10.13a using the FEM, a buckling of a single panel (in between the stiffeners), of the entire panel (whole plate) or a buckling of the stiffener can occur. For the single panel buckling in Figure 10.13c the right partial plate is decisive because it is wider than the left one. While for hand calculations the single panels do not influence each other, for a calculation using the FEM the left panel stabilises the right one and in addition the eigenvalue is increased due to the torsional stiffness of the stiffener, provided that the torsional buckling of the stiffener is not decisive. For a buckling of the entire panel, which is sketched in Figure 10.13d, the stiffener will translate downwards (or upwards). Here, the lateral buckling of the stiffener is of primary importance. If the support of the longitudinal edges has no or only a slight influence, one speaks of a *buckling panel* behaviour "similar to buckling members".

10.10 Verifications for Plate Buckling

Designation plate buckling

The stability problem plate buckling occurs when plates are stressed **in their planes by compression stresses or shear stresses.** These stresses are σ_x, σ_y, τ_{xy} and τ_{yx} of an in-plane loading as shown in Figure 10.3. For that reason, a labelling referring to the loading could have also been chosen. However, since displacements **perpendicular to the plane** emerge for the buckling and since the displacements are chosen for the description of stability problems, as also in the case of beams (lateral buckling, lateral torsional buckling), the designation plate buckling is used due to the "plate deflexion" w(x,y).

Verification methods

For the verification against lateral and lateral torsional buckling of beam members, the following verification methods can be distinguished:

- κ-procedure (see Chapter 9.4 and 9.6)
- Procedure with equivalent geometric imperfections (see Chapter 9.8)
- Plastic zones theory (see Chapter 5.12)

Verifications for **plate buckling** have been conducted with a corresponding modified κ-method so far, since this is regulated in the according engineering standards. As alternative, the method of effective widths becomes more important. A procedure with equivalent geometric imperfections for plates is absolutely imaginable, however, it has not been developed to the point that it could be put into use. There is a lack of appropriate equivalent geometric imperfections as well as of methods for the computation of the stresses and for the verification and load-bearing capacity. Calculations according to the plastic zones theory are also possible for plates, also see [5]. However, they are not adequately regulated for practical issues, especially regulations for the geometric imperfections and the residual stresses to be applied are missing.

For plate buckling, the verifications are usually conducted using the κ-method. For this method, the ideal buckling stresses (eigenvalues) are needed, which are often determined with the help of formulas or diagrams. Since only a limited number of practical cases is covered with these, **the determination of eigenvalues for plate buckling is an important task of the FEM**. Moreover, often the corresponding **eigenmodes** are also needed.

Verification against buckling according to DIN 18800 Part 3

FE-computations have to be executed in a way that the results can be used for buckling verifications going along with the regulations of the standards. Therefore, important principles according to DIN 18800 Part 3 are compiled below.
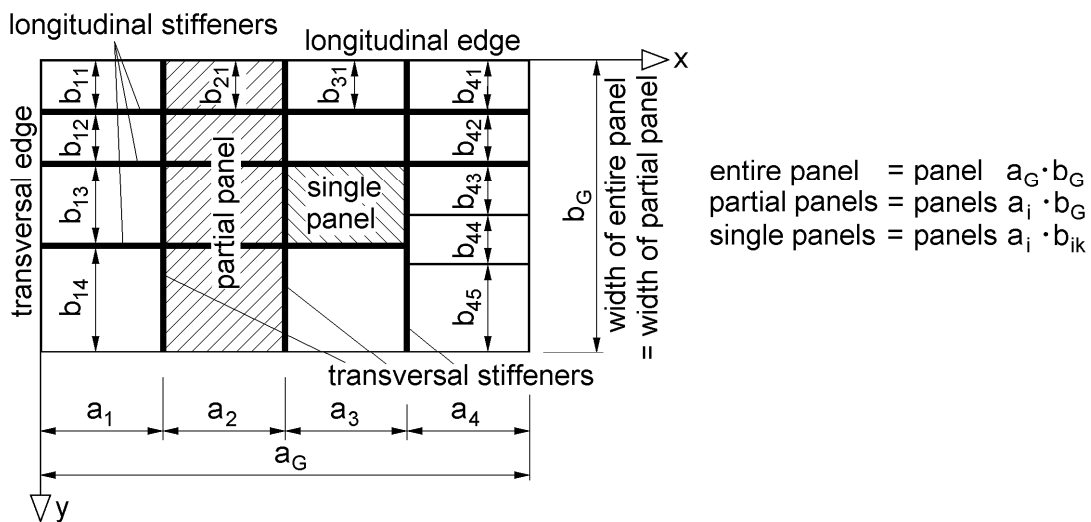

Figure 10.14 Differentiation of different buckling panels, [8]

Rectangular plates of structural components susceptible to buckling are referred to as *buckling panels*. Their longitudinal edges are oriented in the direction of the longitudinal axis of the component. *Buckling panels* can be strengthened by stiffeners. Stiffeners in the direction of the longitudinal edges are longitudinal stiffeners, those in direction of the transverse edges transversal stiffeners.
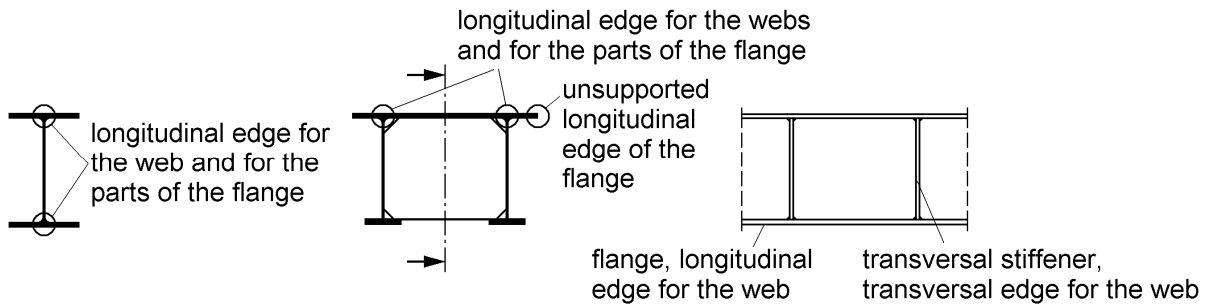
Figure 10.15 Examples for plate edges of webs and parts of the flanges, [8]

As shown in Figure 10.14, buckling panels are differentiated as single, partial and entire panels. Entire panels are stiffened or unstiffened plates, which are generally supported undisplaceably at their logitudinal and transversal edges (see Figure 10.15). The edges can also be supported elastically; longitudinal edges may also be unsupported. Partial panels are logitudinally stiffened or unstiffended plates located in between adjacent transversal stiffeners or between a transverse edge and an adjacent transversal stiffener and the logitudinal edges of the entire panel. The decisive widths of the buckling panels b_G for entire and partial panels and b_{ik} for single panels are defined in Figure 10.16.
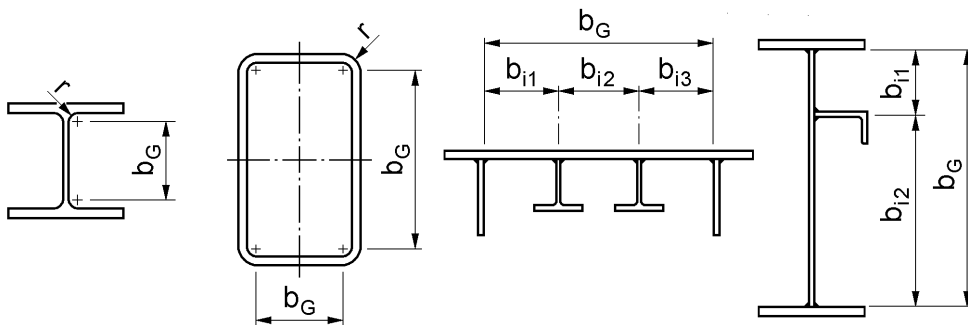

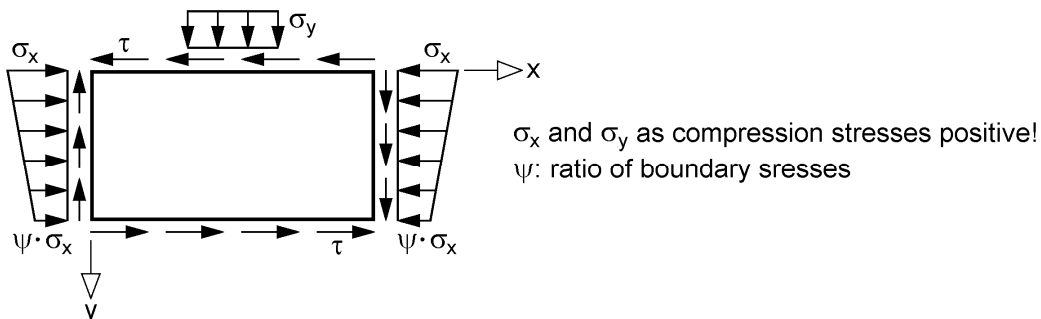**Figure 10.16** Decisive width of the buckling panels, [8]

σ_x and σ_y as compression stresses positive!
ψ: ratio of boundary sresses

Figure 10.17 Stresses σ_x, σ_y and τ in a buckling panel, [8]

DIN 18800 Part 3 contains the following specifications for the assumption of the boundary conditions:

- For plate edges supported perpendicularly to the plate, a hinged support (simple support) is supposed to be assumed.

- For the edges of single panels, which are composed by stiffeners, undisplaceable, hinged bearings may be assumed for the verification of the single panels. For the transversal edges of partial panels, which are composed by transversal stiffeners, undisplaceable bearings may be assumed for the verification of the partial panels.

- For boundary stiffeners, which elastically support a longitudinal edge, an undisplaceable bearing may be assumed, if a stability verification according to DIN 18800 Part 2 is executed for the stiffeners.

- Supporting and fixing effects of the adjacent structural components may be considered if the total stability of the cooperating parts is considered.

Table 10.3   Reduction factos κ for an individual acting of σ_x, σ_y or τ, [8]

Buckling panel	Supports	Stress	Non-dimensional slenderness	Reduction factor
Single panel	At all edges	Axial stresses σ with an edge stress ratio $\psi_T \leq 1$ [*)]	$\overline{\lambda}_p = \sqrt{\dfrac{f_{y,k}}{\sigma_{Pi}}}$	$\kappa = c\left(\dfrac{1}{\overline{\lambda}_p} - \dfrac{0.22}{\overline{\lambda}_p^2}\right) \leq 1$ with $c = 1.25 - 0.12 \cdot \psi_T \leq 1.25$
	At all edges	Shear stresses τ	$\overline{\lambda}_p = \sqrt{\dfrac{f_{y,k}}{\tau_{Pi} \cdot \sqrt{3}}}$	$\kappa_\tau = \dfrac{0.84}{\overline{\lambda}_p} \leq 1$
Partial and entire panel	At all edges	Axial stresses σ with an edge stress ratio $\psi \leq 1$	$\overline{\lambda}_p = \sqrt{\dfrac{f_{y,k}}{\sigma_{Pi}}}$	$\kappa = c\left(\dfrac{1}{\overline{\lambda}_p} - \dfrac{0.22}{\overline{\lambda}_p^2}\right) \leq 1$ with $c = 1.25 - 0.25 \cdot \psi \leq 1.25$
	At three edges	Axial stresses σ	$\overline{\lambda}_p = \sqrt{\dfrac{f_{y,k}}{\sigma_{Pi}}}$ [**)]	$\kappa = \dfrac{1}{\overline{\lambda}_p^2 + 0.51} \leq 1$
	At three edges	Constant edge displacement u	$\overline{\lambda}_p = \sqrt{\dfrac{f_{y,k}}{\sigma_{Pi}}}$ [**)]	$\kappa = \dfrac{0.7}{\overline{\lambda}_p} \leq 1$
	At all edges, without longitudinal stiffeners	Shear stresses τ	$\overline{\lambda}_p = \sqrt{\dfrac{f_{y,k}}{\tau_{Pi} \cdot \sqrt{3}}}$	$\kappa_\tau = \dfrac{0.84}{\overline{\lambda}_p} \leq 1$
	At all edges, with longitudinal stiffeners	Shear stresses τ	$\overline{\lambda}_p = \sqrt{\dfrac{f_{y,k}}{\tau_{Pi} \cdot \sqrt{3}}}$	$\kappa_\tau = \dfrac{0.84}{\overline{\lambda}_p} \leq 1$ if $\overline{\lambda}_p \leq 1.38$ $\kappa_\tau = \dfrac{1.16}{\overline{\lambda}_p^2}$ if $\overline{\lambda}_p > 1.38$

[*)] For single panels ψ_T is the edge stress ratio of the partial panel in which the single panel is located.
[**)] For the determination of σ_{Pi} the buckling value min $k_\sigma(\alpha)$ for $\psi = 1$ is to be regarded.

Table 10.4   Reduction factos κ_σ and κ_τ for panels supported at all edges ($\alpha \geq 1$), [29]

$\overline{\lambda}_P$	Comp., $\psi = 1$[*] b/t			Comp., $\psi \leq 0$[*] b/t for $\psi = 0$			Shear b/t for $\alpha \to \infty$			$\overline{\lambda}_P$	Comp., $\psi = 1$[*] b/t			Comp., $\psi \leq 0$[*] b/t for $\psi = 0$			Shear b/t for $\alpha \to \infty$		
	S235	S355	κ_σ	S235	S355	κ_σ	S235	S355	κ_τ		S235	S355	κ_σ	S235	S355	κ_σ	S235	S355	κ_τ
0.60	33.7	27.6	**1.000**	47.2	38.5	**1.000**	51.3	41.9	**1.000**	1.85	104	85.0	**0.476**	145	119	**0.595**	158	129	**0.454**
0.65	36.6	29.8	**1.000**	51.1	41.7	**1.000**	55.6	45.4	**1.000**	1.90	107	87.3	**0.465**	149	122	**0.582**	162	133	**0.442**
0.70	39.4	32.1	**0.980**	55.0	44.9	**1.000**	59.9	48.9	**1.000**	1.95	110	89.5	**0.455**	153	125	**0.569**	167	136	**0.431**
0.75	42.2	34.4	**0.942**	58.9	48.1	**1.000**	64.1	52.4	**1.000**	2.00	112	91.8	**0.445**	157	128	**0.556**	171	140	**0.420**
0.80	45.0	36.7	**0.906**	62.9	51.3	**1.000**	68.4	55.9	**1.000**	2.05	115	94.1	**0.435**	161	132	**0.544**	175	143	**0.410**
0.85	47.8	39.0	**0.872**	66.8	54.5	**1.000**	72.7	59.4	**0.988**	2.10	118	96.4	**0.426**	165	135	**0.533**	180	147	**0.400**
0.90	50.6	41.3	**0.840**	70.7	57.7	**1.000**	77.0	62.8	**0.933**	2.15	121	98.7	**0.418**	169	138	**0.522**	184	150	**0.391**
0.95	53.4	43.6	**0.809**	74.7	61.0	**1.000**	81.2	66.3	**0.884**	2.20	124	101	**0.409**	173	141	**0.511**	188	154	**0.382**
1.00	56.2	45.9	**0.780**	78.6	64.2	**0.975**	85.5	69.8	**0.840**	2.25	127	103	**0.401**	177	144	**0.501**	192	157	**0.373**
1.05	59.1	48.2	**0.753**	82.5	67.4	**0.941**	89.8	73.3	**0.800**	2.30	129	106	**0.393**	181	148	**0.491**	197	161	**0.365**
1.10	61.9	50.5	**0.727**	86.4	70.6	**0.909**	94.1	76.8	**0.764**	2.35	132	108	**0.386**	185	151	**0.482**	201	164	**0.357**
1.15	64.7	52.8	**0.703**	90.4	73.8	**0.879**	98.4	80.3	**0.730**	2.40	135	110	**0.378**	189	154	**0.473**	205	168	**0.350**
1.20	67.5	55.1	**0.681**	94.3	77.0	**0.851**	103	83.8	**0.700**	2.45	138	113	**0.372**	193	157	**0.464**	210	171	**0.343**
1.25	70.3	57.4	**0.659**	98.2	80.2	**0.824**	107	87.3	**0.672**	2.50	141	115	**0.365**	196	160	**0.456**	214	175	**0.336**
1.30	73.1	59.7	**0.639**	102	83.4	**0.799**	111	90.8	**0.646**	2.55	143	117	**0.358**	200	164	**0.448**	218	178	**0.329**
1.35	75.9	62.0	**0.620**	106	86.6	**0.775**	115	94.3	**0.622**	2.60	146	119	**0.352**	204	167	**0.440**	222	182	**0.323**
1.40	78.7	64.3	**0.602**	110	89.8	**0.753**	120	97.8	**0.600**	2.65	149	122	**0.346**	208	170	**0.433**	227	185	**0.317**
1.45	81.6	66.6	**0.585**	114	93.0	**0.731**	124	101	**0.579**	2.70	152	124	**0.340**	212	173	**0.425**	231	189	**0.311**
1.50	84.4	68.9	**0.569**	118	96.2	**0.711**	128	105	**0.560**	2.75	155	126	**0.335**	216	176	**0.418**	235	192	**0.305**
1.55	87.2	71.2	**0.554**	122	99.5	**0.692**	133	108	**0.542**	2.80	157	129	**0.329**	220	180	**0.411**	239	196	**0.300**
1.60	90.0	73.5	**0.539**	126	103	**0.674**	137	112	**0.525**	2.85	160	131	**0.324**	224	183	**0.405**	244	199	**0.295**
1.65	92.8	75.8	**0.525**	130	106	**0.657**	141	115	**0.509**	2.90	163	133	**0.319**	228	186	**0.398**	248	203	**0.290**
1.70	95.6	78.1	**0.512**	134	109	**0.640**	145	119	**0.494**	2.95	166	135	**0.314**	232	189	**0.392**	252	206	**0.285**
1.75	98.4	80.4	**0.500**	138	112	**0.624**	150	122	**0.480**	3.00	169	138	**0.309**	236	192	**0.386**	257	209	**0.280**
1.80	101	82.7	**0.488**	141	115	**0.610**	154	126	**0.467**	3.05	172	140	**0.304**	240	196	**0.380**	261	213	**0.275**

[*] for partial and entire panels

For the verification against buckling according to DIN 18800 Part 3, reduction ratios κ are required, which can be determined according to Table 10.3. An aid for the determination of κ_σ and κ_τ for panels supported at all edges is given in Table 10.4. The κ-factors are determined using a nondimensional plate slenderness ratio $\overline{\lambda}_P$:

$$\overline{\lambda}_P = \sqrt{\frac{f_{y,k}}{\sigma_{Pi}}} \quad \text{or} \quad \overline{\lambda}_P = \sqrt{\frac{f_{y,k}}{\tau_{Pi} \cdot \sqrt{3}}} \tag{10.44}$$
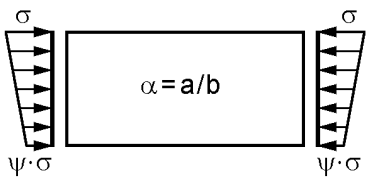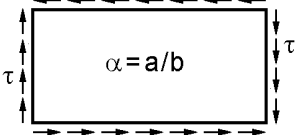
The slenderness ratios depend on the buckling stresses σ_{xPi}, σ_{yPi} and τ_{Pi}, which are to be calculated according to the linear buckling theory. For their calculation, the following assumptions are valid:

- Unlimited validity of *Hooke's* Law
- Ideal isotropic material
- Ideal planarity of the plate
- Ideal centric load application

- No residual stresses
- In equilibrium conditions, only linear terms of displacements are considered.

The ideal buckling stresses are always calculated with σ_x, σ_y or τ acting **individually.** This can be accomplished with the finite element method as shown in Chapter 10.11 and exemplified in Chapter 10.12.

Table 10.5   Buckling values k_σ and k_τ for unstiffened panels with simple, undisplaceable supports at all edges compiled in [29]

Stress	ψ	Aspect ratio $\alpha \geq 1$	Aspect ratio $\alpha < 1$
σ σ $\alpha = a/b$ $\psi \cdot \sigma$ $\psi \cdot \sigma$	$\psi = 1$	$k_\sigma = 4$ (const. compression)	$k_\sigma = \left(\alpha + \dfrac{1}{\alpha}\right)^2 \cdot \dfrac{2.1}{\psi + 1.1}$
	$1 \geq \psi > 0$	$k_\sigma = \dfrac{8.2}{\psi + 1.05}$	
	$0 \geq \psi \geq -1$	$k_\sigma = 7.81 - 6.29 \cdot \psi + 9.78 \cdot \psi^2$	-
	$\psi = -1$	$k_\sigma = 23.9$ (pure bending)	-
	$-1 \geq \psi \geq -2$	$k_\sigma = 5.97 \cdot (1 - \psi)^2$	-
$\alpha = a/b$ τ τ		$k_\tau = 5.34 + \dfrac{4}{\alpha^2}$ $\alpha \to \infty : k_\tau = 5.34$	$k_\tau = 4 + \dfrac{5.34}{\alpha^2}$

Besides computer-oriented solutions, ideal buckling stresses are usually determined with the product of "buckling value times reference stress", that is with buckling values $k_{\sigma x}$, $k_{\sigma y}$ or k_τ (see Table 10.5) and the reference stress σ_e, as shown in the following compilation. In addition, the compilation contains the most important specifications of DIN 18800 Part 3. The subscript P designates the plate buckling.

a, b	Length or width of the analysed *buckling panel*
$\alpha = a/b$	Aspect ratio
t	Plate thickness

$\sigma_e = \dfrac{\pi^2 \cdot E}{12\left(1 - \mu^2\right)}\left(\dfrac{t}{b}\right)^2$ The reference stress σ_e is equal to *Euler's* buckling stress of a plate strip with the length b and the width t, which is supported at both ends free of fixing stresses. Its bending stiffness is replaced by the plate stiffness. With the numeric values $E = 210\ 000$ N/mm^2 and $\mu = 0.3$ it is

$$\sigma_e = 189800\left(\dfrac{t}{b}\right)^2 \dfrac{N}{mm^2} = 1.898 \cdot \left(\dfrac{100 \cdot t}{b}\right)^2 \dfrac{kN}{cm^2}.$$

$k_{\sigma x}$, $k_{\sigma y}$, k_τ Buckling values of the analysed buckling panel with an exclusive acting of the boundary stresses σ_x, σ_y or τ

$\sigma_{xPi} = k_{\sigma x} \cdot \sigma_e$ Ideal buckling stress with an exclusive acting of boundary stresses σ_x

$\sigma_{yPi} = k_{\sigma y} \cdot \sigma_e$ Ideal buckling stress with an exclusive acting of boundary stresses σ_y

$\tau_{Pi} = k_\tau \cdot \sigma_e$ Ideal buckling stress with an exclusive acting of boundary stresses τ

$\lambda_a = \pi \cdot \sqrt{\dfrac{E}{f_{y,k}}}$ The reference slenderness ratio λ_a is calculated with the characteristic material parameters. It is:

$\lambda_a = 92.9$ for St 37 (S 235) with $f_{y,k} = 240$ N/mm^2

$\lambda_a = 75.9$ for St 52 (S 355) with $f_{y,k} = 360$ N/mm^2

$\lambda_P = \pi \cdot \sqrt{\dfrac{E}{\sigma_{Pi}}}$ or $\lambda_P = \pi \cdot \sqrt{\dfrac{E}{\tau_{Pi} \cdot \sqrt{3}}}$ Plate slenderness ratio

$\overline{\lambda}_P = \lambda_P / \lambda_a$ Nondimensional plate slenderness ratio

$\kappa_x, \kappa_y, \kappa_\tau$ Reduction ratios for plate buckling

For stiffened buckling panels, the following cross section and system values are used for the stiffeners:

I Second degree area moment (formerly moment of inertia), calculated with the effective flange width b'

A Area of cross section without effective plate parts

$\gamma = 12\left(1 - \mu^2\right)\dfrac{I}{b_G \cdot t^3}$ Referenced second degree area moment (stiffness); for $\mu = 0.3$ it is $\gamma = 10.92 \cdot \dfrac{I}{b_G \cdot t^3}$

$\delta = \dfrac{A}{b_G \cdot t}$ Referenced cross-sectional area

The effective flange width of stiffeners can be calculated with Figure 10.18 and Table 10.6.
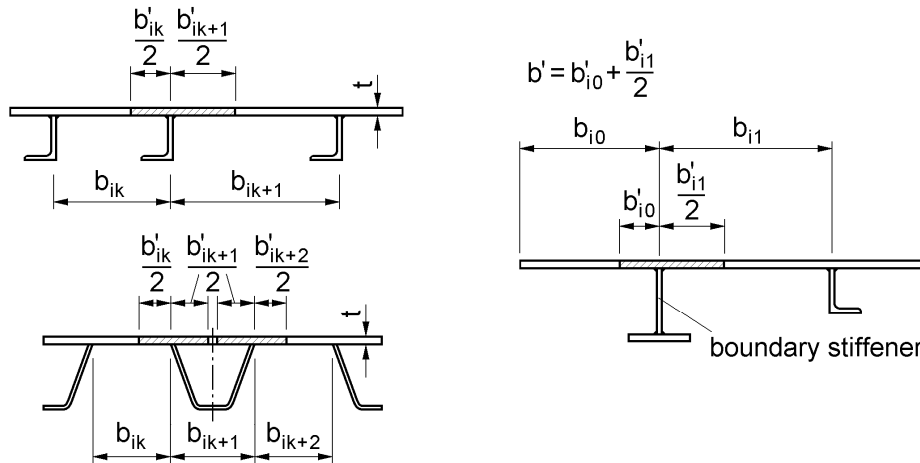
Figure 10.18 Effective flange width of compressed longitudinal and boundary stiffeners, [8]

Table 10.6   Effective flange width of longitudinal stiffeners, [8]

Chord width of		
compressed longitudinal stiffeners	compressed boundary stiffeners	non-compressed longitudinal and boundary stiffeners
$b' = \dfrac{b'_{ik}}{2} + \dfrac{b'_{i,k+1}}{2}$ with $b'_{ik} = 0.605 \cdot t \cdot \lambda_a \cdot \left(1 - 0.133 \cdot \dfrac{t \cdot \lambda_a}{b_{ik}}\right)$ however $b'_{ik} \le b_{ik}$ and $b'_{ik} \le \dfrac{a_i}{3}$	$b' = b'_{i0} + \dfrac{b'_{i1}}{2}$ with $b'_{i0} = 0.138 \cdot t \cdot \lambda_a$ or $b'_{i0} = \dfrac{0.7}{\overline{\lambda}_P} \cdot b_{i0}$ however $b'_{i0} \le b_{i0}$ and $b'_{i0} \le \dfrac{a_i}{6}$	$b'_{ik} = b_{ik}$ however $\le \dfrac{a_i}{3}$ $b'_{i0} = b_{i0}$ however $\le \dfrac{a_i}{6}$

For single, partial and entire panels it is to be verified that the stresses due to the loading do not exceed the limit of the buckling stresses. For an **exclusive** acting of σ_x, σ_y or τ the verifications are to be performed as follows:

$$\frac{\sigma}{\sigma_{P,R,d}} \le 1 \quad \text{with} \quad \sigma_{P,R,d} = \frac{\kappa \cdot f_{y,k}}{\gamma_M} \quad \text{(for } \sigma_x \text{ and } \sigma_y) \tag{10.45}$$

$$\frac{\tau}{\tau_{P,R,d}} \le 1 \quad \text{with} \quad \tau_{P,R,d} = \frac{\kappa_\tau \cdot f_{y,k}}{\sqrt{3} \cdot \gamma_M} \tag{10.46}$$

If stresses σ_x, σ_y and τ occur simultaneously, the verification has to be performed according to element 504 of DIN 18800 Part 3 (also see [61] and [75]). However, this case is not shown here, since it does not have great relevance in practice. In this context the combination of σ_x and τ is more interesting, for which the following verification condition is valid:

$$\left(\frac{|\sigma_x|}{\sigma_{xP,R,d}}\right)^{e_1} + \left(\frac{\tau}{\tau_{P,R,d}}\right)^{e_3} \le 1 \tag{10.47}$$
$$\text{with: } e_1 = 1 + \kappa_x^4 \text{ and } e_3 = 1 + \kappa_x \cdot \kappa_\tau^2$$

With Eq. (11.34), the ideal buckling stresses σ_{xPi} and τ_{Pi} have do be determined for an individual acting of σ_x and τ as mentioned previously. Further regulations of DIN 18800 Part 3 shall not be responded to at this point, however, it should be mentioned that the following points are of special importance:

- Behaviour of the *buckling panel* "similar to buckling members"
- Structural design of stiffened plates and compressed stiffener requirements
- Interaction of plate buckling with lateral buckling

For a quick estimation of the resistance of unstiffened panels, Figure 10.19 contains an evaluation of the verification conditions for different stress states. Using the panel ratio b/t, the figure allows a direct determination of the maximum possible stress for the following cases:

- max σ_x with $\tau = 0$
- max σ_x with $\tau = 5$ kN/cm^2
- max σ_x with $\tau = 10$ kN/cm^2
- max τ with $\sigma_x = 0$

The evaluation for max τ has been performed with $k_\tau = 5.34$ (a/b $\rightarrow \infty$), $k_\tau = 6.34$ (a/b = 2) and $k_\tau = 9.34$ (a/b = 1) according to Table 10.5. For max σ_x with $\tau = 5$ and 10 kN/cm^2, the value $k_\tau = 5.34$ is regared, which is min k_τ.
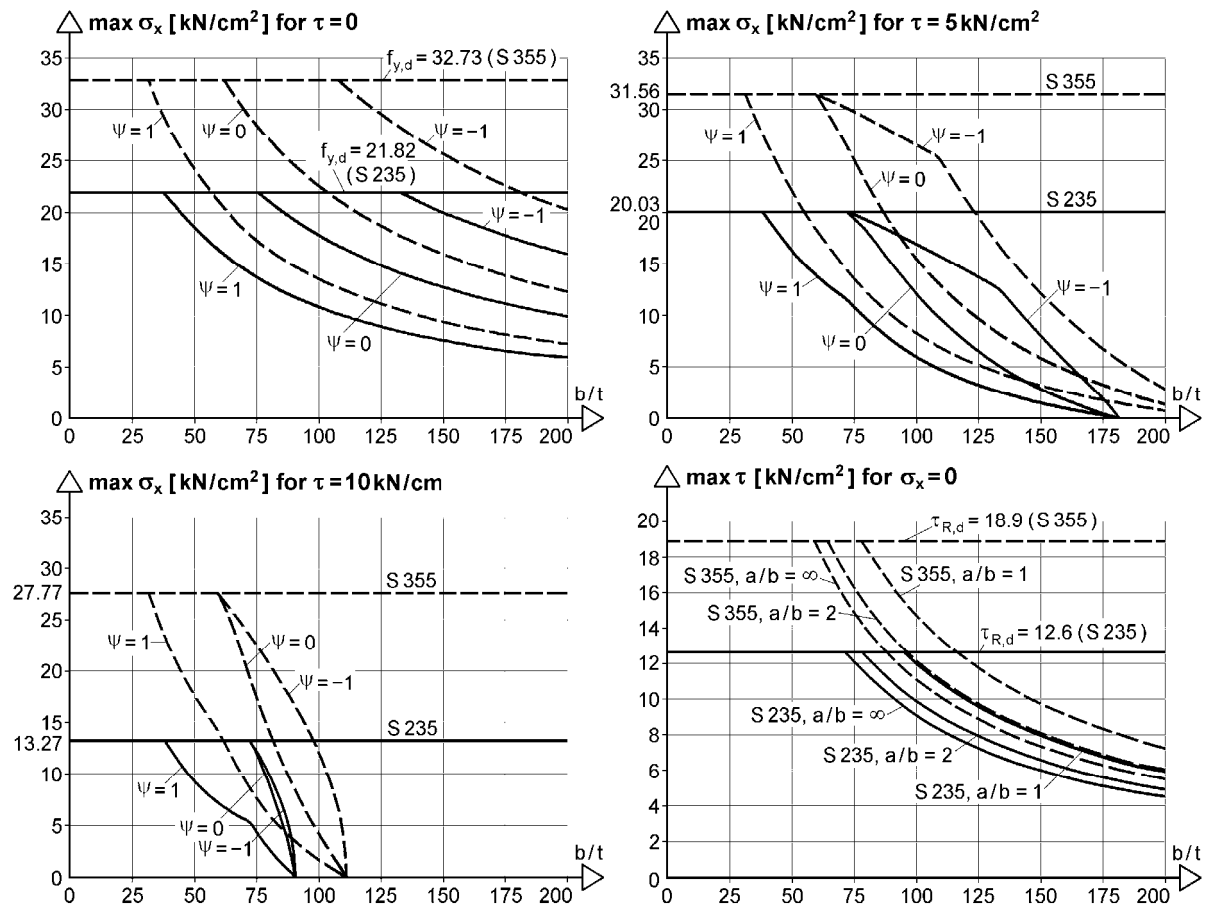
Bild 10.19   Maximum stresses for unstiffened partial and entire panels supported at all sides regarding κ according to Table 10.3

**Verification against buckling according to
DIN Technical Report 103/Eurocode 3**

The DIN Technical Report 103, Steel Bridges [11], is valid for motorway bridges and railway bridges and replaces the present national regulations for these bridges. Basis of the technical report is Eurocode 3 [10] or its status when the technical report was published, respectively. The guideline of DIN Technical Report 103, Steel Bridges [81], contains comments and calculation examples which should make the application of the technical report easier.

For plate buckling, two methods are regulated in [11], see [81] as well:

1. A procedure where the stress of a beam is devided into longitudinal stresses, shear stresses and transversal stresses due to the loads at the transversal edges. For each stress component, an individual verification against buckling is conducted. For the consideration of the mixed stress state, the verifications are then combined using in interaction relationships. **This procedure works** with **effective cross sections** regarding the longitudinal stresses.

2. A **procedure with a limitation of stresses**, where the limit loading is determined for each buckling panel of the cross section regarding the mixed stress state, for which the contribution of the total cross section is applied.

According to [11], the procedure with a limitation of stresses is usually to be used for the **design of steel bridges.** This procedure and its methodology widely comply with DIN 18800 Part 3, as long as the individual acting of the stresses σ_x, σ_y and τ is analysed. The corresponding buckling values can be determined with appropriate tables or with **computer calculations (FEM)**.

For the combination of stresses σ_x, σ_y and τ acting, the *von Mises* criterion (equivalent stress) is used as boundary condition in [11]. In the notation of [81], it is:

$$\left(\frac{\sigma_{x,Ed}}{\sigma_{x,Rd}}\right)^2 + \left(\frac{\sigma_{y,Ed}}{\sigma_{y,Rd}}\right)^2 - \left(\frac{\sigma_{x,Ed}}{\sigma_{x,Rd}}\right)\cdot\left(\frac{\sigma_{y,Ed}}{\sigma_{y,Rd}}\right) + \left(\frac{\tau_{Ed}}{\tau_{Rd}}\right)^2 \leq 1.0 \qquad (10.48)$$

The boundary stresses $\sigma_{x,Rd}$, $\sigma_{y,Rd}$ and τ_{Rd} are determined with buckling curves and the coaction is regarded in the system slenderness

$$\bar{\lambda}_P = \sqrt{\frac{\alpha_{ult,k}}{\alpha_{crit}}} \qquad (10.49)$$

The amplification factor α_{crit} is the bifurcation load factor η_{Ki} for the combined acting of the stresses σ_x, σ_y and τ. For the determination of α_{crit}, an **FEM-analysis** or an appropriate solution from the corresponding literature can be used. The execution of the verifications is dealt with using the example of Chapter 10.12.2.

10.11 Determination of Buckling Values and Eigenmodes with the FEM

In this chapter, the determination of buckling values and eigenmodes is covered with the help of finite elements. Using the matrices in Chapters 10.7 to 10.9, the stiffness matrix $\underline{K}$ and geometric stiffness matrix $\underline{G}$ can be set up for the buckling panels. With these, a homogeneous matrix equation yields for the eigenvalue problem "plate buckling":

$$(\underline{K} + \eta_{Pi,r} \cdot \underline{G}) \cdot \underline{v}_r = 0 \tag{10.50}$$

In Eq. (10.50), $\eta_{Pi,r}$ is the *bifurcation load factor for plate buckling*, which is required for the calculation of buckling values or ideal buckling stresses. $\underline{v}_r$ is the eigenvector, with which the eigenmode (buckling shape) is described. The subscript "r" designates the number of the eigenvalue.

In Chapter 6 the determination of eigenvalues and eigenmodes is dealt with in detail regarding the buckling of beam structures. Since Eq. (10.50) is formally in accordance with Eq. (6.30), the method suggested in Chapter 6.2 can also be used for plate buckling, i. e. the combination of a *matrix decomposition method* with the *inverse vector iteration* is recommended. The iterative calculation can be structured according to Chapter 6.2.5 as follows:

1. Search for interval
   (matrix decomposition)

2. Reduction of interval
   (matrix decomposition)

3. Determination of bifurcation load factor and eigenmode
   (*inverse vector iteration*)

4. Check

In comparison to the beam structures, three fundamental differences can be recognised for plate buckling:

- The band width of the matrix equation (10.50) is often significantly larger, so that the complexity (calculating time) for the matrix decomposition increases considerably in comparison to the vector iteration.

- In many cases, not only the 1st eigenvalue is needed for plate buckling but higher eigenvalues as well. In Chapter 10.12.2, the buckling of the entire panel corresponds to the 11th eigenvalue for example.

- The eigenvalues are located very close to each other for plate buckling. For that reason, the solution method must be modified accordingly.

For plate buckling it is necessary to determine the searched eigenvalue r with relative high accuracy using the matrix decomposition method. Since the eigenvalues can be very close together, the decomposition should be executed until an exactness of approximately 0.001 is reached. Afterwards, the inverse vector iteration can be started, as described in Chapter 6.2.4. It serves the determination of the eigenvectors and the exact eigenvalues. As initial value η_0, the approximated eigenvalue of the matrix decomposition is used and with that the vector iteration is displaced to the area of the searched eigenvalue (*spectral displacement*). As a general principle, the following is valid: The closer the initial value is located to the searched eigenvalue and the more the start vector and the eigenvector are alike, the faster the vector iteration converges to the right solution. As discussed in Chapter 6.2.4, the use of a start vector generated using random numbers is recommended for plate buckling as well. In [2], it is suggested to set all elements of the start vectors to the value one.

In order to determine the eigenmode correctly, the inverse vector iteration should generally be conducted until the exactness of the eigenvalue is of at least 10^{-5}. Afterwards, the check described in Chapter 6.2.5 has to be carried out. If more than one eigenvalue is located in the considered interval, it can be reduced. However, as shown in Chapter 10.12.1, this is useless if several equal eigenvalues occur. The procedure of the calculations is explained with the following example. Here, the case is also covered when the vector iteration does not converge to the searched eigenvalue and eigenvector.

Example:

For the stiffened buckling plate in Figure 10.23, the 11th eigenvalue and the corresponding eigenmode are to be determined. According to Chapter 10.12.2, this is buckling of the entire panel. This case results for the chosen partition with 20×16 finite elements as 11th eigenvalue. With a different partition into elements, the buckling of the entire panel could for example also be the 10th eigenvalue. With the FE-calculation, one obtains:

$$10^{th} \text{ eigenvalue:} \quad \eta_{Pi,10} = 2.8353$$

$$11^{th} \text{ eigenvalue:} \quad \eta_{Pi,11} = 2.9531$$

$$12^{th} \text{ eigenvalue:} \quad \eta_{Pi,12} = 2.9922$$

As it can be seen, the 10th and the 12th eigenvalue are close to the 11th eigenvalue (96.0 % or 101.3 %), so that an exactness of 0.001 is reasonable for the determination of the eigenvalues with the matrix decomposition method. With this, the decomposition is carried out 13 times for the search of the 11th eigenvalues, that is for the following values of η: 1; 5; 3; 2; 2.5; 2.75; 2.875; 2.9375; 2.9688; 2.9531; 2.9453; 2.9492; 2.9512.

As a result of the interval reduction, it is found out that the 11th eigenvalue searched is located between 2.9512 and 2.9531. If the following vector iteration is started with

the mean value of the interval range, i. e. a spectral displacement of $\eta_0 = 2.9521$ is conducted, one obtains $\eta_{Pi,11} = 2.95311$ after some iterations with an exactness allowance of 10^{-5}.

The number of the required iterations depends on the choice of the start vector. Even though random numbers were assigned to it, the vector iteration also converges for this example using different random start vectors always after six iteration steps. The concluding check with the matrix decomposition method for $\eta_u = 0.9999 \cdot 2.95311$ and $\eta_o = 1.0001 \cdot 2.95311$ shows that the 11th eigenvalue is the only one located in the interval. For this reason, it is clearly verified that the eigenvector, which is determined with the vector iteration, belongs to the 11th eigenvalue. This is not self-evident, since the vector iteration can also converge to the next higher or lower eigenvalue and eigenvector. If the check shows that the searched eigenvalue has not been found, the exactness of the matrix decomposition method can be increased to 0.0001. Another possibility is a different vector iteration with a correspondingly changed initial value η_o. In the case that previously the next higher eigenvalue has been determined, a smaller initial value has to be chosen, where at minimum the lower boundary determined with the reduction of the interval has to be used. Since the eigenvector is needed anyway, the last method stated is to be preferred.

FE-modelling of buckling panels

As a general rule, it is sufficient to divide *buckling panels* into plate elements of equal size. However, the partition has to consider the location of longitudinal and transversal stiffeners, i. e. the element borders have to be arranged at these positions. The number of plate elements to be chosen in longitudinal and transverse direction depends on the specific problem. In general, the degrees of freedom, which arise due to the discretisation, have to be able to describe the modal shape in a proper way. For that reason, the calculated eigenmode should always be inspected in order to ascertain whether it shows many waves which can be covered with the chosen partition into elements or not. 10 to 20 plate elements in longitudinal direction and 5 to 20 in transverse direction are a reasonable choice for many structural problems.

10.12 Examples of Applications for Plate Buckling

In the following examples, compression stresses are assumed to be positive as in DIN 18800 Part 3. When using computer programs, it has to be paid attention to whether tension or compression stresses are defined as positive. The following FE-calculations are conducted with the *RUBSTAHL*-program *BEULEN*, also see Chapter 1.10.

10.12.1   Single Panel with Constant σ_x and $\alpha \approx 1,5$

The buckling panel shown in Figure 10.20 is analysed and the smallest eigenvalue as well as the respective eigenmode determined. The buckling panel is part of the track system girders for the magnetic levitation train Transrapid, which was built some years ago in large quantities for the Transrapid testing facility in Emsland [37]. According to [80], it was further developed concerning structural aspects afterwards. The middle part of the cover plate between the webs of the main girder and the transverse compartment is analysed with the assumption of simple supports at the edges of the buckling panel.
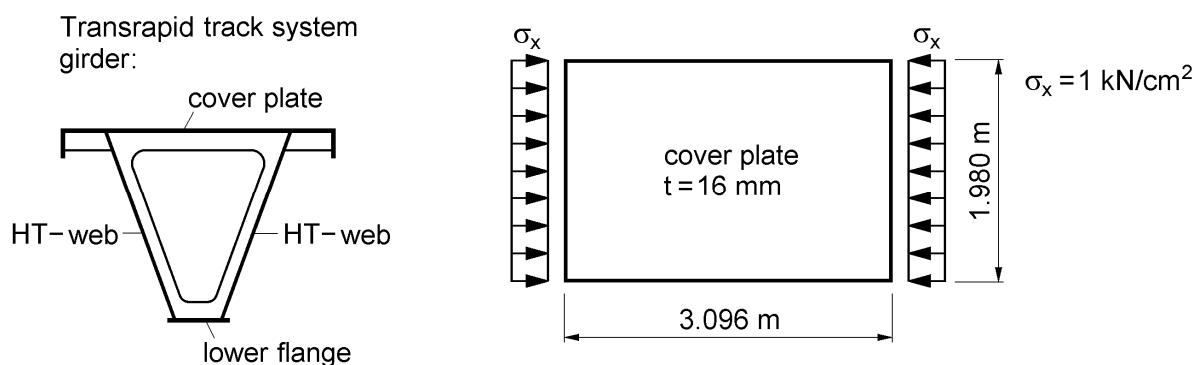
Figure 10.20 Buckling panel of the cover plate of a Transrapid track system girder

Since the aspect ratio of the *buckling panel* is larger than 1, the ideal buckling stress is usually calculated with the buckling value $k_\sigma = 4.0$. With the reference stress

$$\sigma_e = 1.898 \cdot \left(\frac{100 \cdot 1.6}{198} \right)^2 = 1.239 \cdot \frac{kN}{cm^2} \tag{10.51}$$

it follows

$$\sigma_{Pi} = 4.0 \cdot 1.239 = 4.956 \cdot kN \big/ cm^2 . \tag{10.52}$$

Due to the large number of the girders, the buckling value was calculated more precisely. It is generally known that with an aspect ratio of $\alpha = \sqrt{2} = 1.41$ the **single-**

waved eigenmode turns into a **two**-waved. The buckling value $k_\sigma = 4.50$ corresponds to $\alpha = \sqrt{2}$ according to [42] and with $\alpha = 1.564$ for the buckling panel regarded here the buckling value is:

$$k_\sigma = \left(\frac{2}{1.564} + \frac{1.564}{2} \right)^2 = 4.247 \tag{10.53}$$

The ideal buckling stress is then $\sigma_{Pi} = 5.262 \text{ kN/cm}^2$, which is 6.2 % larger than the one with $k_\sigma = 4.0$.

For comparison this value is calculated with an FE-program. As shown in Figure 10.21, the buckling panel is divided into 10×10 finite elements with a total of 100 elements. The figure also shows the numbering of the elements and nodes and furthermore the boundary conditions for the simple supports (*Navier's* support). As a result of the FEM analysis, one obtains the bifurcation load factor $\eta_{Pi} = 5.264$ and the buckling value $k_\sigma = 4.248$ with, as expected, the **two-waved** eigenmode shown in Figure 10.22. The second eigenvalue is by the way $\eta_{Pi} = 6.016$ or $k_\sigma = 4.854$ and has a **single-waved** buckling shape.
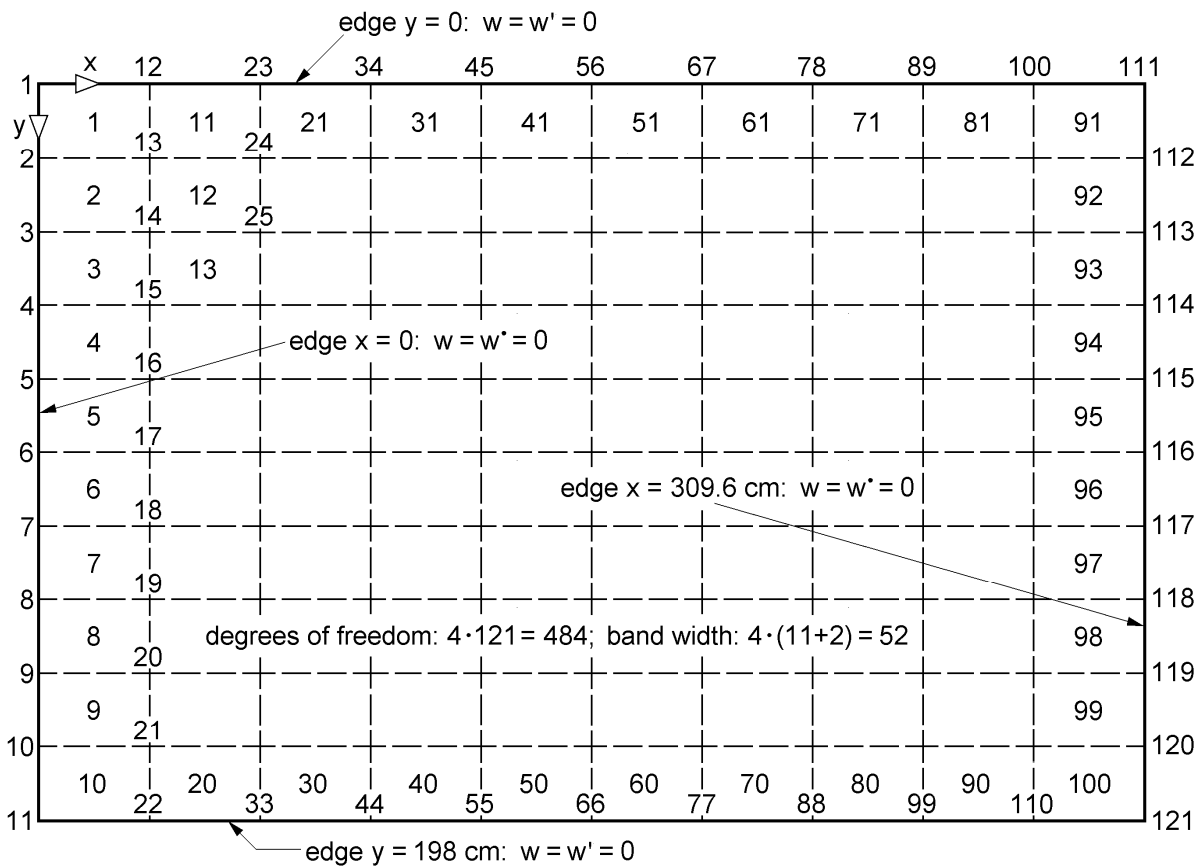
Figure 10.21 FE-modelling of the buckling panel in Figure 10.20
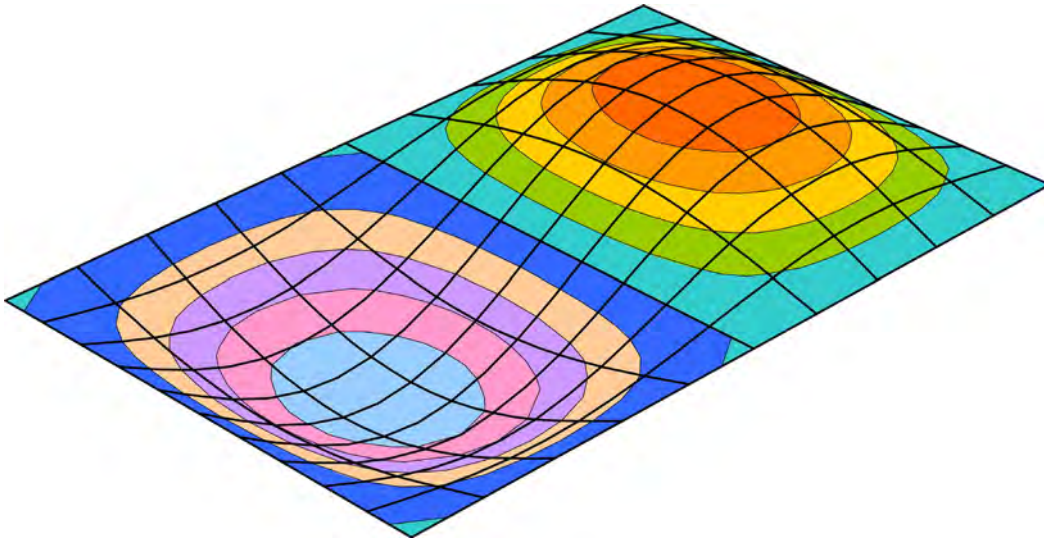
Figure 10.22 Two-waved modal shape at the first eigenvalue

With $\sigma_{Pi} = 5.262$ kN/cm^2 and $f_{y,k} = 24.0$ kN/cm^2, the non-dimensional slenderness is

$$\bar{\lambda}_P = \sqrt{\frac{f_{y,k}}{\sigma_{Pi}}} = \sqrt{\frac{24.0}{5.262}} = 2.136 \tag{10.54}$$

and the reduction ratio κ according to DIN 18800 part 3 (table 1, line 1):

$$\kappa = (1.25 - 0.12) \cdot \left(\frac{1}{2.1369} - \frac{0.22}{2.136^2} \right) = 0.475 \tag{10.55}$$

For the limit compression stress, it is

$$\sigma_x \leq 0.475 \cdot 24.0/1.1 = 10.36 \text{ kN/cm}^2. \tag{10.56}$$

Due to the postcritical reserve bearing capacities, a compression stress is permitted which is clearly larger than the ideal buckling stress.

Variant with $\alpha = \sqrt{2}$

As a variation to the buckling panel of Figure 10.20, the case of an aspect ratio α equal to $\sqrt{2}$ is now regarded. For a better understanding of eigenvalue calculations, the corresponding buckling panel is shown in Figure 10.23.

As already mentioned above, the transition from a single to a two-waved buckling shape is at $\alpha = \sqrt{2}$ and the first and second eigenvalue are equal:

$$\sigma_{x,Pi,1} = \sigma_{x,Pi,2} = 4.50 \cdot \sigma_e = 8.541 \text{ kN/cm}^2. \tag{10.57}$$

An FEM-analysis with a 10×10 mesh leads to $\eta_{Pi} = 8.54182$, a value which complies with the theoretical solution within the scope of the computation exactness. The
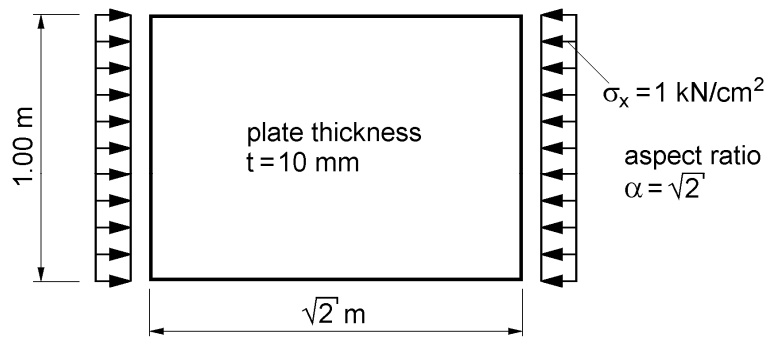
Figure 10.23 Buckling panel with σ_x const. and $\alpha = \sqrt{2}$

check described in Chapter 10.11 shows that the intervals 0.9999 η_{Pi} to 1.0001 η_{Pi} include two eigenvalues, namely the first and second one. Even if the interval is arbitrarily reduced, this result does not change. Therefore, the question is whether the FE-calculation leads to a eigenmode belonging to the first or the second eigenvalue. This basically depends on the programming. Since the initial value η_0 for the vector iteration is of significant impact, with $\eta_0 < \eta_{Pi}$, one usually obtains a eigenmode which belongs to the first eigenvalue. In contrast to that, it is most likely that for $\eta_0 > \eta_{Pi}$, the eigenmode will correspond to the second eigenvalue. The vector iteration will only lead to the other eigenvalue if the start vector strongly tends to the buckling shape of this eigenvalue. Even if it is often clear which eigenvalue the eigenmode corresponds to (as in this example), with mathematic means this can only be determined with big efforts. Computer programs require a corresponding programming.

10.12.2 Beam Web with Longitudinal Stiffeners

The buckling panel shown in Figure 10.24 is analysed in [62] in detail, calculating the buckling values with the help of formulas. Here, they are determined with a FE-program and the longitudinal stiffeners are regarded as in [62]: A = 8.73 cm^2, I = 410 cm^4 and $I_T = I_\omega = 0$.
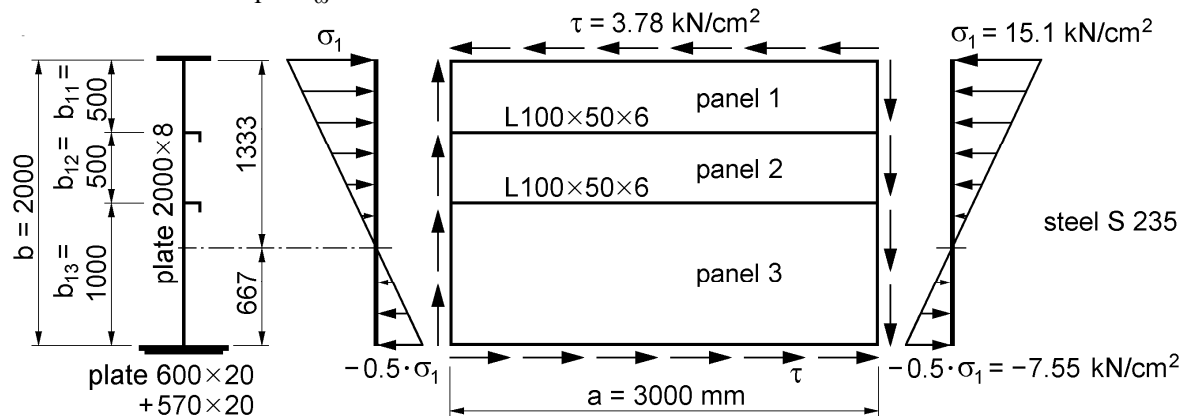

Figure 10.24 Beam web with longitudinal stiffeners

For the FE-calculation, the *buckling panel* is divided into $20 \times 16 = 320$ equal plate elements. A look into the design aid of Figure 10.19 shows that the **buckling panel without longitudinal stiffeners** is not able to carry the existing stresses. This is also by trend confirmed by very small ideal buckling stresses, which result to $\sigma_{1Pi} = 4.1656 \text{ kN/cm}^2$ (eigenmode with two longitudinal waves) and to $\tau_{Pi} = 2.1471 \text{ kN/cm}^2$ (eigenmode with a large diagonal wave) according to the finite element method. The longitudinal stiffeners are therefore necessary.

The FE-calculation of the **buckling panel with longitudinal stiffeners** leads to $\eta_{Pi} = 1.7993$ as **1$^{\text{st}}$ eigenvalue for the axial stress** and $\sigma_{1Pi} = 27.1693 \text{ kN/cm}^2$. The buckling of single panel 1 is decisive since the buckling shape shows seven half waves there and the others only have small deflexions. A comparative analysis for an isolated single panel being simply supported at all edges leads to $\sigma_{1Pi} = k_\sigma \cdot \sigma_e = 8.2/(0.625 + 1.05) \cdot 4.86 = 23.79 \text{ kN/cm}^2$. This value is smaller than $\sigma_{1Pi} = 27.25 \text{ kN/cm}^2$ because in the FE-calculation the stiffening (supporting) effect of panels 2 and 3 are taken into consideration.

For the calculation of the 2$^{\text{nd}}$ to 10$^{\text{th}}$ eigenvalue, bifurcation load factors between 1.7995 and 2.8323 occur. The buckling shapes with 6 to 13 distinct waves within panel 1 show that this panel is decisive. Partially, also large amplitudes result in panel 2. The **buckling of the entire panel** does not occur until the 11$^{\text{th}}$ eigenvalue with $\eta_{Pi} = 2.9531$ and $\sigma_{1Pi} = 44.59 \text{ kN/cm}^2$ is reached, for which the stiffeners show a lateral deflexion. The eigenmode is shown in Figure 10.25. For the buckling of the entire panel, the example in Chapter 10.11 contains additional calculation results and explanations. In [62], $\sigma_{1Pi} = k_\sigma \cdot \sigma_e = 77.9 \cdot 0.304 = 23.7 \text{ kN/cm}^2$ and after a tightening of the calculation, $\sigma_{1Pi} = 98.5 \cdot 0.304 = 29.9 \text{ kN/cm}^2$ are determined with formulas or using the tables for buckling values of [47], respectively. The difference to the FE-computation of 33 % is significant and the formulas of [62] are apparently well on the safe side.
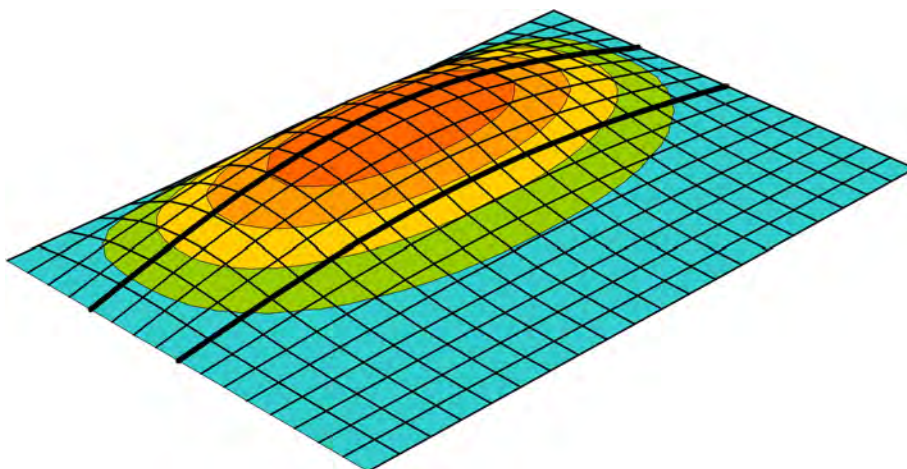

Figure 10.25 Buckling of the entire panel in Figure 10.23 for σ_x (11$^{\text{th}}$ eigenvalue)

For the exclusive acting of the shear stresses one obtains $\eta_{Pi} = 1.8941$ and $\tau_{Pi} = 7.1599$ kN/cm^2 (1st eigenvalue) using an FE-calculation. The buckling shape is located in panel 3 and shows two diagonal waves. Panel 3 is decisive for shear buckling as also mentioned in [62] and there the corresponding ideal buckling stress is determined with $\tau_{Pi} = 23.2 \cdot 0.304 = 7.05$ kN/cm^2, a value, which complies with the FE-result. The verifications for structural safety are not shown here since they are shown in [62] in detail.

DIN Technical Report 103

The buckling panel of Figure 10.23 is also treated in [81] and on 29 (!) pages different approaches for the verification are analysed. Here, it is compared with the calculations in Chapter II-3.4 of [81] and the factor α_{crit} is calculated with the help of the FEM.

If the first eigenvalue is calculated with the FE-program "Beulen" regarding the acting of σ and τ, it leads to $\eta_{Pi} = \alpha_{crit} = 1.705$ and a buckling shape which shows six distinct waves (longitudinal) in panel 1 and small amplitudes in panels 2 and 3. The first eigenvalue therefore corresponds to the **buckling of single panel 1**, for which an amplification factor $\alpha_{crit} = 1.52$ is calculated in [81]. The corresponding hand calculation is relatively time-consuming, so that the use of an FE-program provides advantages. Moreover, the value 1.705 is larger (12 %) and more exact than $\alpha_{crit} = 1.52$, since in comparison to the hand calculation, the FE-analysis takes into account the stiffening (supporting) effect of the adjacent panels. This effect has already been pointed out at the beginning of the chapter.

For the investigation of the buckling of the entire panel, the following values are taken as a basis in [81]:

$$\sigma_{1Pi} = k_\sigma \cdot \sigma_e = 77.90 \cdot 0.304 = 23.68 \text{ kN/cm}^2 \tag{10.58}$$

$$\tau_{Pi} = k_\tau \cdot \sigma_e = 23.2 \cdot 0.304 = 7.05 \text{ kN/cm}^2 \tag{10.59}$$

With these ideal buckling stresses, an amplification factor $\alpha_{crit} = 1.17$ for the combined acting of σ and τ is determined. While the value for τ_{Pi} is relatively exact, σ_{1Pi} is comparatively far on the safe side, so that α_{crit} must be larger than 1.17.

A determination of α_{crit} with an FE-program is relatively difficult since the buckling of the entire panel has to be identified visually on the basis of the eigenmode. This is made even more difficult due to the acting of σ and τ. Because the eigenvalues 1 to 5 show five to nine distinct waves in panel 1, they are to be associated with a single panel buckling. The 6th eigenvalue leads to a long waved eigenmode, which is indeed irregular, as shown in Figure 10.26, but it totally covers the upper stiffener. $\eta_{Pi,6} = 1.984 = \alpha_{crit}$ is determined as 6th eigenvalue, a value significantly larger than 1.17 according to [81] (see above).
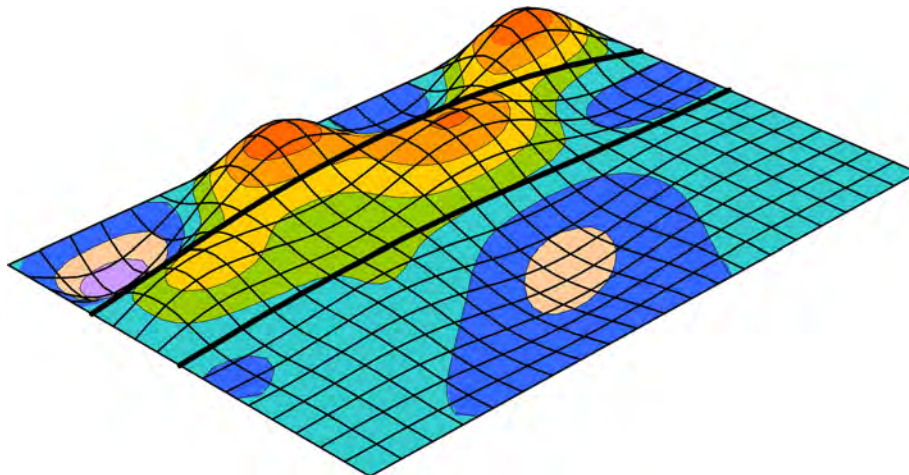
Figure 10.26 Eigenmode shape for the acting of σ and τ (6th eigenvalue)

The result should therefore be checked using the ideal buckling stresses regarding the individual effect. With the values of the FE-computation specified above, one obtains:

$$\alpha_{crit,\sigma} = \frac{44.59}{15.1} = 2.95 \tag{10.60}$$

$$\alpha_{crit,\tau} = \frac{7.16}{3.78} = 1.89 \tag{10.61}$$

For the combined acting of both of the stresses a α_{crit} usually results which is smaller than the lower single value. In the case that both single values are far apart (which is the case here), α_{crit} is slightly smaller than the lower single value. Therefore, a value of about $\alpha_{crit} = 1.8$ would be expected here, so that the FE-result seems to be inconsistent. However, an examination shows that the $\alpha_{crit,\tau} = 1.89$ belongs to the shear buckling in panel 3 and that tension stresses act there which lead to a decrease of the danger of buckling.

For the analysis of the buckling of the entire panel it is often reasonable to roughly subdivide the buckling panel into finite elements and to arrange element borders only in the range of the stiffeners. Therefore, the buckling panel of Figure 10.23 is now divided transversally into 4 and longitudinally into 20 elements. With this, the first eigenvalue represents a buckling of the entire panel for which the upper stiffener shows a lateral deflexion and with $\eta_{Pi} = 1.936$, a value which tends to confirm $\eta_{Pi,6} = 1.984$ (see above).

10.12.3   Web Plate of a Composite Bridge with Shear Stresses

In Figure 10.27, the web plate of a composite bridge at the bridge end is shown. Axial stresses are small and therefore the plate buckling due to shear stresses is examined

only. For the calculation with the FEM, the web plate is divided into 10 identical plate elements in longitudinal and transverse direction.
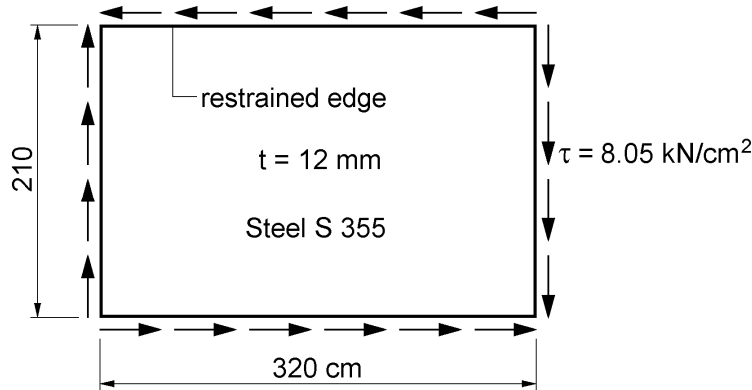

Figure 10.27 Web plate of a composite bridge

If a simple support is assumed for each edge of the buckling panel, as it is common practice, the calculation with the FEM leads to $\tau_{pi} = 4.357$ and the *modal shape* mainly shows a large, diagonal wave. A computation leads to:

$$k_\tau = 5.34 + \frac{4}{(320/210)^2} = 7.063 \tag{10.62}$$

$$\sigma_e = 1.898 \cdot \left(\frac{100 \cdot 1.2}{210}\right)^2 = 0.6197 \ \text{kN}/\text{cm}^2 \tag{10.63}$$

$$\tau_{Pi} = 7.063 \cdot 0.6197 = 4.377 \ \text{kN}/\text{cm}^2 \tag{10.64}$$

The verification for the structural safety according to DIN 18800 Part 3 with this ideal buckling stress reveals that the existing shear stress can not be carried. However, the assumed support at the upper edge is on the safe side since the concrete slab is adjacent there. Due to the structural design between the concrete slab and the web plate, a restraint can be applied at the upper edge of the buckling panel. The calculation with the FEM then leads to $\tau_{Pi} = 5.528$ kN/cm^2, a value which is 27 % larger than for the simple support. An adequate structural safety can now be verified according to DIN 18800 Part 3:

$$\bar{\lambda}_P = \sqrt{\frac{36}{5.528 \cdot \sqrt{3}}} = 1.939 \tag{10.65}$$

$$\kappa_\tau = \frac{0.84}{1.939} = 0.433 \tag{10.66}$$

$$\Rightarrow \frac{8.05}{0.433 \cdot 36/(\sqrt{3} \cdot 1.1)} = \frac{8.05}{8.182} = 0.984 < 1 \tag{10.67}$$

10.12.4 Web Plate with High Bending Stresses

The example of Chapter 10.12.3 is continued here and the bending stresses within the field range of the composite bridge are examined. At the upper edge of the web, axial compression stresses occur and at the lower edge, due to the bending moment and the asymmetric cross section of the bridge, high tensile stresses occur, see Figure 10.28.
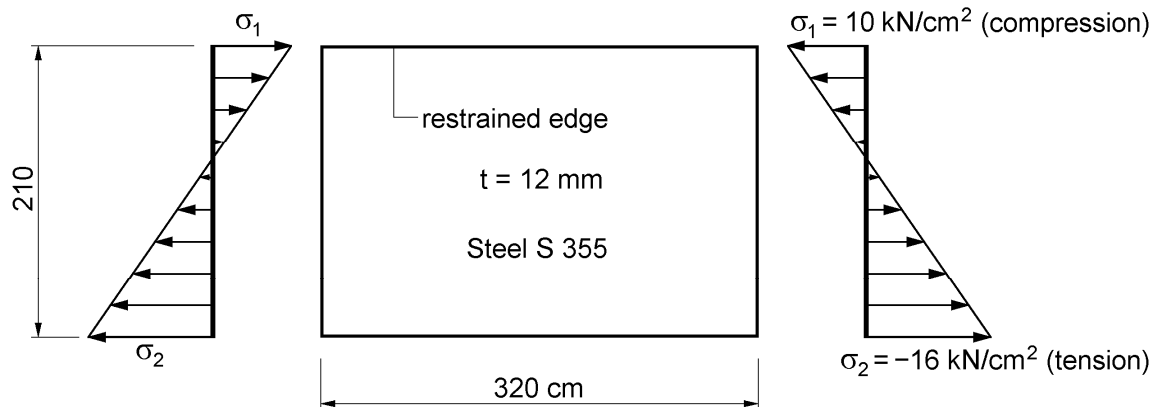

Figure 10.28 Web plate with high bending stress

An FE-calculation with a restrained upper edge as described in Chapter 10.12.3 leads to $\eta_{Pi} = 4.1614$ and $\sigma_{1P,i} = 41.614$ kN/cm^2. The corresponding eigenmode shows **four waves in longitudinal direction**, which are concentrated in the upper part of the buckling panel due to the compression stress. Whether the existing loadings can be carried, shall not be discussed here. With this example priority is given to the evaluation of the calculation results.

A computer program could possibly determine $\eta_{Pi} = -0.6352$ as result of the calculation. The minus sign of the bifurcation load factor can easily be missed. If it is detected, an inexperienced user could be irritated and concludes that the program calculates incorrectly. This view could be strengthened with the consideration of the corresponding *buckling shape*. In the case the program provides and displays the eigenmode, it could have **two waves** in longitudinal direction being strongly developed in the lower area of the buckling panel. This described case can occur if the computer program uses the inverse vector iteration as solution method, since it determines the smallest absolute eigenvalue. In the example regarded here, the **first negative eigenvalue** of $\eta_{Pi} = -0.6352$ is located closer to the origin of the iteration with $\eta = 1$ than the **first positive eigenvalue** with $\eta_{Pi} = (+)4.1614$. Using the inverse vector iteration, the first positive eigenvalue can only be determined, if, as described in the Chapters 10.11 and 6.2.4, a *spectral displacement* close to the first positive eigenvalue is carried out. This should of course be done by the program and it should be ensured by corresponding checks (point 4 in Chapter 6.2.5). However, one can also input higher stresses and cause a spectral displacement. If stresses three times as

big as those in Figure 10.28 are entered, one is closer to the first **positive** eigenvalue than to the first **negative** one.

Kindmann, R. / Kraus, M.

Steel Structures
Design using FEM
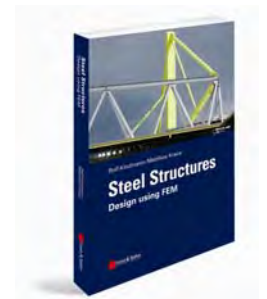
This book presents the design of steel structures using finite element methods (FEM)according to the current state of the art in Germany and the rest of Europe. After a short introduction on the basics of the design, this book illustrates the FEM with a focus on internal forces, displacements, critical loads and modal shapes. Next to finite element procedures for linear calculations considering the stress states of normal force, biaxial bending and warping torsion, non-linear calculations and the stability cases of flexural buckling, lateral torsional buckling and plate buckling are concentrated on significantly. In this context, design procedures for stability according to the standard Eurocode 3 is introduced and discussed. In addition, important fundamental issues are covered, such as the determination of cross-section properties as well as the elastic and plastic cross-section resistance. Complementary, finite element procedures for cross sections are dealt with, which will have an increasing importance in the future.

This book has evolved within the teaching activities of the authors in the lecture Computer-oriented Design of Steel Structures on the Masters Programme Computational Engineering at the University of Bochum. It covers the total variety of demands needed to be discussed for the safe, economic and modern design of steel structures.

Die Finite-Elemente-Methode (FEM) bildet heute in der Praxis der Bauingenieure ein Standardverfahren zur Berechnung von Tragwerken. Nach einer Einführung in die Methodik konzentriert sich das Buch auf die Ermittlung von Schnittgrößen, Verformungen, Verzweigungslasten und Eigenformen für Stahlkonstruktionen. Neben linearen Berechnungen für Tragwerke bilden die Stabilitätsfälle Biegeknicken, Biegedrillknicken und Plattenbeulen mit der Ermittlung von Verzweigungslasten und Berechnungen nach Theorie II. Ordnung wichtige Schwerpunkte. Hinzu kommt die Untersuchung von Querschnitten, für die Berechnungen mit der FEM zukünftig stark an Bedeutung gewinnen werden. Für praktisch tätige Ingenieure und Studierende gleichermaßen werden alle notwendigen Berechnungen für die Bemessung von Tragwerken anschaulich dargestellt.

Fax-Answer on +49(0)30 47031 240 - Ernst & Sohn, Berlin

Number	Order-No..	Titel	Unit price
	978-3-433-02978-7	Steel Structures	€ 59,-
	905765	Publishing Index Verlag Ernst & Sohn	For free
	2092	Journal Stahlbau	For free

Delivery- and Invoice address:　　　☐privat　　　　☐business

Company	
Contact person	Telephone
UST-ID Nr./VAT-ID No.	Fax
Street/No.	E-Mail

Country	-	Zip code	Location

Date/Signature